Computers and Chemical Engineering 84 (2016) 132–150

Contents lists available at ScienceDirect

Computers and Chemical Engineering

journal homepage: www.elsevier.com/locate/compchemeng

Population balance discretization for growth, attrition, aggregation, breakage and nucleation

Diego Bertin*, Ivana Cotabarren, Juliana Piña, Verónica Bucalá

Department of Chemical Engineering – Universidad Nacional del Sur (UNS), Planta Piloto de Ingeniería Química (PLAPIQUI) – UNS-CONICET, Camino La Carrindanga Km. 7, 8000 Bahía Blanca, Argentina

ARTICLE INFO

Article history:
Received 10 December 2014
Received in revised form 14 August 2015
Accepted 18 August 2015
Available online 28 August 2015

Keywords:
Population balance equation
Particles size distribution
Discretization method
Size change mechanisms

ABSTRACT

This paper presents a new discretization method to solve one-dimensional population balance equations (PBE) for batch and unsteady/steady-state continuous perfectly mixed systems. The numerical technique is valid for any size change mechanism (i.e., growth, aggregation, attrition, breakage and nucleation occurring alone or in combination) and different discretization grids.

The developed strategy is based on the moving pivot technique of Kumar and Ramkrishna and the cell-average method of Kumar et al. A novel contribution is proposed to numerically handle the growth and attrition terms, for which a new representation of the number density function within each size class is developed. This method allows describing the number particle fluxes through the class interfaces accurately by preserving two sectional population moments.

By comparing the numerical particle size distributions with analytical solutions of one-dimensional PBEs (including different size change mechanisms and particle-size dependent kinetics), the accuracy of the proposed numerical method was proved.

1. Introduction

Particulate systems play an important role in a wide variety of industrial processes (among others: mining, food processing, pharmaceuticals and fertilizers manufacture). Changes in particle size distributions (PSDs) often take place in these industries due to different mechanisms, which can occur either alone or in combination, such as aggregation, growth, breakage, attrition and nucleation (Gerstlauer et al., 2006; Ramkrishna, 2000).

An appropriate modeling approach for quantify PSDs is the concept of population balance equation (PBE), which was developed several decades ago (Hulburtz and Katz, 1964). Ramkrishna (2000) defined the PBE as an equation to describe the density of a suitable extensive variable, usually the particle number (in terms of the number density function), so that the PBE represents a number balance on particles of a specific state. Significant efforts were those of Hulburtz and Katz (1964), Randolph and Larson (1971) and Ramkrishna (2000) to formalize a generic PBE capable of quantifying the different mechanisms by which particles of a specific state can either appear in or disappear from the system. Mathematically the PBE corresponds to a non-linear partial integro-differential equation, which presents only very few analytical solutions for some ideal cases. On the other hand, numerical solutions require substantial computational resources because, in practical engineering processes, PSDs may extend over several orders of magnitude and can be very sharp (Vanni, 2000; Qamar, 2008). Moreover, some methods exhibit lack of stability and accuracy of the solution. Since there is a great variety of processes that are studied by means of modeling and simulation (processes design, control and optimization), there is still need of numerical methods development to solve those mathematical models that include PBEs (Pinto et al., 2008; Utomo et al., 2009).

Several numerical methods have been proposed/used in the literature to solve PBEs, among others, the methods of: moments (Hulburtz and Katz, 1964; Motz et al., 2002; Madras and McCoy, 2004; Marchisio and Fox, 2005; Bajcinca et al., 2014), characteristics (Kumar and Ramkrishna, 1997; Pilon and Viskanta, 2003; Qamar and Warnecke, 2007), finite differences/discretization (Marchal et al., 1988; Hounslow et al., 1988; Kumar and Ramkrishna, 1996a,b; Ma et al., 2002) and Monte Carlo (Smith and Matsoukas, 1998; Kruis et al., 2000; Lee and Matsoukas, 2000; Lin et al., 2002). Frequent problems related to the numerical solution of PBEs include, among others, the inaccurate calculation of the PSD for strong aggregation processes, numerical instabilities for growth processes and stiffness of the equations system for rapid particle nucleation (Maurstad, 2002; Kiparissides, 2006).

* Corresponding author. Tel.: +54 291 486 1700x268; fax: +54 291 486 1600.
E-mail address: dbertin@plapiqui.edu.ar (D. Bertin).

http://dx.doi.org/10.1016/j.compchemeng.2015.08.011
0098-1354/

Nomenclature

A	attrition rate (m/s)
b	breakage rate (s^{-1})
b_0	constant in the breakage rate in Eq. (106) ($m^{-1}\ s^{-1}$)
b'_0	constant in the breakage rate in Eq. (129) ($m^{-3}\ s^{-1}$)
B_{nuc}	discrete nucleation rate (s^{-1})
C_{1i}	parameter for the linear approximation in Eq. (45) (m^{-2})
C_{2i}	parameter for the linear approximation in Eq. (45) (m^{-1})
d_p	particle diameter (m)
$d_{p_{crit}}$	critical diameter in Case 3 (m)
d_{p_i}	mean diameter in class i (m)
d_{nuc}	diameter of particles born by nucleation (m)
d_{nv}	number–volume mean diameter (m)
D_{p_i}	lower node in class i (m)
$\bar{D}_{p_i}$	arithmetic mean diameter in class i (m)
$\bar{D}^A_{p_i}$	average diameter of particles born by aggregation in class i (m)
$\bar{D}^B_{p_i}$	average diameter of particles born by breakage in class i (m)
$\bar{D}^B_{p_{j\to i}}$	average diameter of particles born by breakage in class i from class j (m)
$\bar{D}^{in}_p$	average diameter of particles of class i in the inlet flowrate (m)
G	growth rate (m/s)
G_0	constant in Eq. (82) (m^{1-q}/s)
G'_0	constant in Eq. (93) (m/s)
G''_0	constant in Eq. (119) (s^{-1})
h^{A+}	particle birth rate by aggregation ($m^{-1}\ s^{-1}$)
h^{A-}	particle death rate by aggregation ($m^{-1}\ s^{-1}$)
h^{B+}	particle birth rate by breakage ($m^{-1}\ s^{-1}$)
h^{B-}	particle death rate by breakage ($m^{-1}\ s^{-1}$)
H_i^{A+}	flow of particles born by aggregation in class i (s^{-1})
H_i^{A-}	flow of particles dead by aggregation in class i (s^{-1})
H_i^{B+}	flow of particles born by breakage in class i (s^{-1})
H_i^{B-}	flow of particles dead by breakage in class i (s^{-1})
I_0	modified Bessel function of the first kind of order zero
I_1	modified Bessel function of the first kind of order one
k	index of summation in Eqs. (76) and (77)
n	number density function (m^{-1})
n_0	number density function (m^{-1})
n_i	discrete number density function in class i (m^{-1})
$\dot{n}_{in}$	number density function of the particles entering the system ($m^{-1}\ s^{-1}$)
$\dot{n}_{nuc}$	rate of number density function of particles by nucleation ($m^{-1}\ s^{-1}$)
$\dot{n}_{out}$	number density function of the particles leaving the system ($m^{-1}\ s^{-1}$)
N_0	initial total particle number
N_i	particle number in class i
$\dot{N}_{i_{in}}$	inlet number flow rate of particles in class i
$\dot{N}_{i_{nuc}}$	flow of particles born by nucleation in class i (s^{-1})
$\dot{N}_{i_{out}}$	outlet number flow rate of particles in class i
p	exponent in Eq. (82)
P	breakage probability function (m^{-1})
q	index of the conserved population moment
$Q_{attrition}$	volume flow rate leaving the particles population by attrition (m^3/s)
Q_{growth}	volume flow rate fed to the system which contributes to the particle growth (m^3/s)
Q_{in}	inlet volumetric flow rate (m^3/s)
Q_{out}	outlet volumetric flow rate (m^3/s)
r	geometric grid ratio between classes
S	total particle surface area (m^2)
V	total particle volume (m^3)
V_0	initial total particle volume (m^3)
t	time (s)
T	dimensionless time
x	integration variable (m)
x'	integration variable (m)
x''	integration variable (m)

Greek letters

α_i	parameter defined in Eq. (52)
β	aggregation kernel (s^{-1})
γ_i	parameter defined in Eq. (57)
δ	Dirac delta function
λ	half width of the pulse defined in Eq. (96) (m)
Γ	Gamma function
μ_j	jth population moment (m^j)
μ_{j_i}	jth sectional population moment in class i (m^j)
$\bar{\mu}$	arithmetic mean diameter of the PSD (m)
μ_0	arithmetic mean diameter of the initial PSD (m)
ν	average number of particles formed by breakage
σ_0	standard deviation of the initial PSD (m)
τ	mean residence time (s)

Subscripts

i	class of the discrete PSD
j	class of the discrete PSD
k	class of the discrete PSD

In particular, discretization techniques have been one of the most popular numerical methods. They consist in dividing the continuous range of particle specific state (usually the particle size) into discrete classes and discretizing the density function in the domain of the internal coordinate by concentrating the particles within each class on a mean class size. Several discretization methods are available in the literature, which basically differ in the choice of the discretization grid and the global population properties that are conserved (Hounslow et al., 1988; Kumar and Ramkrishna, 1996a,b; Vanni, 2000; Nopens et al., 2005).

Hounslow et al. (1988) developed a discretization procedure for growth, nucleation and aggregation processes, limited to the use of a geometric grid. Vanni (2000) extended that method to breakage processes. Kumar and Ramkrishna (1996a) also developed a discretization method (called the fixed pivot technique) to solve PBEs for batch systems with aggregation and breakage, which is capable to predict desired global properties of the PSDs by using an arbitrary discretization grid. Although results of fixed pivot technique proved to be generally very accurate for estimating PSDs, the method failed to correctly predict the PSDs for aggregation processes in large size ranges represented on a coarse geometric grid. Then, Kumar and Ramkrishna (1996b) developed a new discretization technique to overcome this problem by defining moving pivots that concentrate the particle number of a given size range.

Kumar et al. (2006) developed a numerical procedure for solving PBEs for batch aggregation processes that guarantees the exact conservation of two population properties of interest. This technique (called the Cell Average Technique) involves the computation of the average size of newborn particles by aggregation and their

assignment to neighboring existing grid classes. The proposed method, for any kind of grid, solves the overprediction in the large size range given by the fixed pivot technique (Kumar and Ramkrishna, 1996a).

For processes involving growth/attrition mechanisms (convective flows), the PBE exhibits partial derivatives and thus the equation is hyperbolic. It is known that hyperbolic equations present several difficulties in obtaining accurate numerical solutions (LeVeque, 2002). One of the main challenges for a numerical scheme is to capture the steep moving fronts that may appear in the PSD. A simple strategy is to use finite differences to approximate the involved derivatives (Durran, 2010). However, classical finite difference approaches are not recommended for the PBE numerical solution because its hyperbolic nature often leads to broadening of the sharp discontinuities due to numerical diffusion (Mesbah et al., 2009). Numerical diffusion acts similarly to physical diffusion, smoothing sharp gradients in the final solution. It is also well known that first order finite difference schemes show numerical diffusion. On the other hand, higher order schemes reduce numerical diffusion but tend to introduce numerical dispersion that causes unphysical oscillations. Second (or higher) order methods induce numerical dispersion through the odd-order terms in the truncation error (Sweby, 1984).

In recent years, high-resolution methods have emerged as an interesting option for solving PBEs containing convective flow. These techniques aim to obtain high accuracy on coarse grids, solving sharp discontinuities in order to avoid both numerical diffusion and dispersion (Qamar et al., 2007). To achieve this, the discretized growth and attrition terms are conditioned by a function called flux limiter that tends to high order accuracy in the PSD smooth region and a first order scheme is used in the vicinity of large gradients. Hence, these methods are effective in reducing numerical diffusion present in first order discretization and also in eliminating the oscillations caused by higher order discretization schemes (Gunawan et al., 2004). Although these methods have proven to be accurate, high-resolution methods still require high computational time (Majumder et al., 2010), limiting their application to optimization and control problems that require the PBE solution many times to find optimal operating conditions or control parameters.

Another numerical technique to solve the PBE with growth and/or attrition is the Method of Characteristics (MOC), which is based on the Lagrangian approach, i.e., on the description of each particle along its characteristic in the particle size-time plane. MOC allows lumping the accumulation and convective flow terms within the material derivative (Qamar and Warnecke, 2007). Then, the PBE (partial differential equation) becomes a system of two ordinary differential equations along the characteristic curves. This mathematical structure avoids the numerical diffusion/dispersion errors caused by the growth/attrition term discretization (Kumar and Ramkrishna, 1997).

Due to the several serious difficulties like numerical diffusion and dispersion, inaccuracy and restriction to non-generic grids, it is very difficult to recognize the best method for a general growth/attrition problem (Ramkrishna, 2000). The more sophisticated methods available in the literature are more complicated to implement and difficult to couple with other conservation balances (Kumar, 2006).

The different discretization techniques, which are simple to implement and then widely used, still present problems to handle the growth/attrition term. These methods typically allow calculating the desired global properties of the particles' distribution accurately (Hounslow et al., 1988; Kumar and Ramkrishna, 1997). However the PSD may be subject to severe errors, in fact the calculated PSDs frequently exhibit non-physical oscillations that give negative particle number values in some classes, or deviate from the exact solution due to numerical diffusion at the discontinuous moving fronts (Mesbah et al., 2009).

Most of the existing numerical methods to solve PBEs were derived for specific size change mechanisms (Hounslow et al., 1988; Marchal et al., 1988; Qamar, 2008; Ramkrishna, 2000). The aim of this work is the development of a numerical method, appropriate to solve PBEs defined by only one internal coordinate, having the following main features:

- Appropriate to model batch or unsteady/steady-state continuous perfectly mixed systems.
- Valid for any size change mechanism (i.e., nucleation, growth, aggregation, attrition and breakage occurring alone or in combination).
- Applicable to any type of grid.
- Neither requires the reassignment of newborn particles to predefined sizes nor the addition or subtraction of size classes over time.
- Preserves two population moments exactly: the total number of particles (or moment 0) and an arbitrary moment μ_q (i.e., 0 and q are the conservated population moment indexes) for each grid class and then for the entire population.
- Provides accurate PSDs prediction.
- Simple implementation.

The proposed method extends the moving pivot technique of Kumar and Ramkrishna (1996b) developed for aggregation and breakage, by using a cell-average property for newly born particle redistribution. Besides, a simple strategy (based on an upwind linear scheme) is developed to minimize the above-mentioned problems caused by the growth/attrition term discretization.

2. Theory

For a perfectly mixed system and one internal coordinate (particle diameter, d_p), the PBE is given by (Ramkrishna, 2000):

$$\frac{\partial n(d_p,t)}{\partial t} = -\frac{\partial}{\partial d_p}[G(d_p)n(d_p,t)] + \frac{\partial}{\partial d_p}[A(d_p)n(d_p,t)] + \dot{n}_{in} - \dot{n}_{out} + h^{A+} - h^{A-} + h^{B+} - h^{B-} + \dot{n}_{nuc} \quad (1)$$

For the formulation of Eq. (1), it is implicitly assumed that a number density of particles $n(d_p, t)$ exists at every point of the particle size domain (Ramkrishna, 2000).

In Eq. (1), G and A represent the growth and attrition rates, respectively, and $\dot{n}_{in}$ and $\dot{n}_{out}$ are the number density function flows associated to the particles entering and leaving the system, respectively. h^{A+} and h^{A-} are the source and loss terms of the number density function by aggregation, respectively. Similarly, h^{B+} and h^{B-} are the source and loss terms of the number density function by breakage, respectively. Finally, $\dot{n}_{nuc}$ is the rate of nucleation for the number density function.

In order to completely define the PBE formulation given by Eq. (1), initial and boundary conditions are required. The initial condition for the time domain is:

$$n(d_p, 0) = n_0(d_p) \quad (2)$$

where $n_0(d_p)$ represents the initial PSD within the system. The following boundary condition is considered (Rigopoulos and Jones, 2003):

$$n(0, t) = 0 \quad (3)$$

For the density function $n(d_p, t)$, the jth population moment μ_j is defined as (Randolph and Larson, 1971):

$$\mu_j = \int_0^\infty n(d_p, t) d_p^j dd_p \tag{4}$$

Population moment balances are macroscopic equations derived from the integration of the microscopic PBE. In fact, if Eq. (1) is multiplied by d_p^j and integrated with respect to d_p in the entire size domain (i.e., between zero and infinity), the balance for the jth moment is given by:

$$\frac{d\mu_j}{dt} = -\int_0^\infty \frac{\partial}{\partial d_p}[G(d_p)n(d_p, t)]d_p^j dd_p + \int_0^\infty \frac{\partial}{\partial d_p}[A(d_p)n(d_p, t)]d_p^j dd_p + \int_0^\infty (\dot{n}_{in} - \dot{n}_{out} + h^{A+} - h^{A-} + h^{B+} - h^{B-} + \dot{n}_{nuc})d_p^j dd_p \tag{5}$$

While PBEs allow determining the PSDs changes, the macroscopic balances (also called moment equations) allow calculating the population global properties (or moments), such as the total particle number (N), surface (S) or volume (V). In the moment equations, the internal coordinate gradients are not involved. For example, for a one-dimensional PBE, only the time remains as independent variable (Cameron et al., 2005). The loss of detail of the moment equations with respect to PBEs greatly simplifies the mathematical description and solution; however, inherent information regarding the population distribution is lost (Ramkrishna, 2000).

Commonly, only the first population moments are of interest. In fact, considering d_p as internal coordinate, μ_0 represents the total particle number of the population, while μ_2 and μ_3 are proportional to the total particle surface and volume, respectively (Hounslow et al., 1988). In particular, for spherical particles these moments are given by (Allen, 2003):

$$\pi\mu_2 = S \tag{6}$$

$$\frac{\pi}{6}\mu_3 = V \tag{7}$$

where S and V are the total particle surface and volume, respectively.

The equations that describe the rate of change of the moments are commonly used to evaluate the accuracy of the PSDs calculated by solving PBEs numerically. The procedure involves the comparison of the population moments estimated by using the predicted PSDs (by numerical evaluation of Eq. (4)) with the corresponding values calculated from macroscopic balances given by Eq. (5) (Randolph and Larson, 1971; Hounslow et al., 1988), as the process time evolves.

Before introducing the novel numerical technique proposed to solve the PBE, the terms of Eq. (1), that represent different size change mechanisms, are below described.

2.1. Growth

In this work, growth is defined as the gradual particle size enlargement by coating, being mathematically represented by the first term of the right-hand side of Eq. (1). This mechanism is a size change phenomenon that can occur in granulation processes, and it is characterized by the particle growth through deposition of successive liquid droplets (i.e., of binder) or fine powder on the solids surface (Smith and Nienow, 1983; Kayaert and Antonus, 1997; Mörl et al., 2007).

Growth is a number-conserving but mass-increasing process that shifts the PSD toward larger sizes (Bucalá and Piña, 2007). The growth rate (G), which describes the differential growth of the particles, is defined as:

$$G(d_p) = \frac{dd_p}{dt} \tag{8}$$

where $G(d_p) \geq 0$. If Eq. (5) is used to evaluate μ_3 for spherical particles and the particle flux goes to zero at the boundary $d_p \to 0$, by comparison of its first term of the right-hand side with the mass balance, the growth term must satisfy:

$$\frac{\pi}{2}\int_0^\infty G(d_p)n(d_p, t)d_p^2 dd_p = Q_{growth} \tag{9}$$

where Q_{growth} is the volumetric flowrate fed to the system contributing to particle growth.

2.2. Attrition

The attrition term is used to denominate all the gradual particle size reduction mechanisms, such as physical erosion (Rhodes, 2008) or surface chemical reaction (Wang et al., 2003; Leturia, 2013). Attrition is a number-conserving and mass-decreasing process that shifts the PSD toward smaller sizes. The attrition rate is defined as:

$$A(d_p) = -\frac{dd_p}{dt} \tag{10}$$

Since attrition reduces the particle size, $A(d_p) \geq 0$. Analogously to the growth term, when attrition takes place the following equation must be satisfied:

$$\frac{\pi}{2}\int_0^\infty A(d_p)n(d_p, t)d_p^2 dd_p = Q_{attrition} \tag{11}$$

where $Q_{attrition}$ is the material volume flowrate leaving the particles' population due to attrition.

2.3. Aggregation

The mechanism of aggregation, agglomeration or coalescence refers to the successful collision of two particles to give a new composite particle (Qamar, 2008). During each aggregation event, the total particle volume remains conserved while the total particle number decreases (Bucalá and Piña, 2007). In granulation processes, the aggregation rate is usually a function of the particles' and binder's physical properties, the particle size and operating conditions (Cameron et al., 2005).

Aggregation terms are given as follows (Ramkrishna, 2000):

$$h^{A+}(d_p, t) = \frac{1}{2}\int_0^\infty \int_0^\infty \beta(x, x')n(x, t)n(x', t)\delta\left[x' - (d_p^3 - x^3)^{\frac{1}{3}}\right] \times \left(\frac{\partial x'}{\partial d_p}\right) dx' dx \tag{12}$$

$$h^{A-}(d_p, t) = \int_0^\infty \beta(d_p, x)n(d_p, t)n(x, t)dx \tag{13}$$

where $h^{A+}(d_p, t)$ and $h^{A-}(d_p, t)$ denote the particle "birth" and "death" rates by aggregation in each size d_p. $\beta(x, x')$ is called the aggregation kernel and describe the frequency of aggregation between a particle of size x and another one of size x'. $\beta(x, x')$ relates the aggregation probability with operating conditions and particles' size and physical properties of both particles and binder (Abberger, 2001; Cameron et al., 2005). Because of the limited knowledge of the phenomena that underlie aggregation,

most of the proposed aggregation kernels are empirical or semi-empirical and involve unknown fitting parameters (Ramachandran and Barton, 2010).

In Eq. (12), $\delta(x' - (d_p^3 - x^3)^{1/3})$ is the Dirac delta function, which has a null value for every size except for $x' = (d_p^3 - x^3)^{1/3}$, where its value is infinitely large. $(\partial x'/\partial d_p) = [(d_p^3 - x^3)^{-2/3} d_p^2]$ is the Jacobian that transforms the particle density function with respect to coordinates x and x' into one in terms of d_p (Ramkrishna, 2000). By using the integration property of the Dirac delta function, Eq. (12) can be simplified to:

$$h^{A+}(d_p, t) = \frac{1}{2}\int_0^\infty \beta\left[x, (d_p^3 - x^3)^{\frac{1}{3}}\right] n(x,t) n\left[(d_p^3 - x^3)^{\frac{1}{3}}\right] \times \left[(d_p^3 - x^3)^{-\frac{2}{3}} d_p^2\right] dx \quad (14)$$

2.4. Breakage

Breakage refers to the generation of fragments from existing particles by, for example, mechanical fracture (Ramkrishna, 2000). The breakage terms are given as follows:

$$h^{B+}(d_p, t) = \int_0^\infty \nu(x) b(x) P(d_p, x) n(x, t) dx \quad (15)$$

$$h^{B-}(d_p, t) = b(d_p) n(d_p, t) \quad (16)$$

where $h^{B+}(d_p, t)$ and $h^{B-}(d_p, t)$ represent the particle birth and death rates by breakage, respectively. $b(x)$ is the breakage rate and describes the frequency of breakage for a particle of size x and $\nu(x)$ is the average number of particles generated by breakage of a single particle of size x. $P(d_p, x)$ is the breakage probability function, which describes the number density of particles of size d_p produced from the breakage of particles of size x. This function represents the size distribution for the fragments born by breakage and must satisfy the following normalization condition (Ramkrishna, 2000):

$$\int_0^x P(d_p, x) dd_p = 1 \quad (17)$$

Besides, since $P(d_p, x)$ must be null for $x < d_p$, the integration interval in Eq. (15) can be rewritten as:

$$h^{B+}(d_p, t) = \int_{d_p}^\infty \nu(x) b(x) P(d_p, x) n(x, t) dx \quad (18)$$

According to the breakage probability function $P(d_p, x)$, the number of fragments originated from the breakage of a single particle of size x is given as (Ramkrishna, 2000):

$$\nu(x) = \frac{x^3}{\int_x^0 P(d_p, x) d_p^3 dd_p} \quad (19)$$

For breakage processes, the total volume of particles is conserved while the total number of particles increases (Bucalá and Piña, 2007). The description of processes involving size reduction of particulate solids through PBEs is still the subject of many experimental as well as theoretical works (Holdich, 2002).

2.5. Nucleation

Nucleation refers to the formation of new particles from a liquid or fine powder feed (Cameron et al., 2005). Nucleation leads to the birth of small particles providing the initial stage for further growth or aggregation mechanisms.

Although nucleation is sometimes considered just a boundary condition (Ramkrishna, 2000), as suggested by other authors here it is represented by an additional PBE term (Hounslow et al., 1988; Kumar and Ramkrishna, 1997; Gunawan et al., 2004). Assuming born particles of equal size, $\dot{n}_{nuc}$ in Eq. (1) is represented by:

$$\dot{n}_{nuc} = B_{nuc} \delta(d_p - d_{nuc}) \quad (20)$$

B_{nuc} is the nucleation rate and d_{nuc} is the size of the particles born by nucleation. For $d_{nuc} > 0$, nucleation increases both the total number and mass of the population particles. Although Eq. (20) only includes particles of one size, it can be used more than once in the PBE if the particles born by nucleation have different diameters.

3. Numerical method

As described earlier, the discretization methods divide the entire domain of particles size into small cells or classes, where each class i corresponds to the size interval defined as $[D_{p_i}, D_{p_{i+1}}]$. Here, a representative size d_{p_i} $(D_{p_i} \le d_{p_i} < D_{p_{i+1}})$ is proposed to concentrate the particle number of the class i in a single size value. Thus, the density function within class i can be mathematically represented as (Kumar and Ramkrishna, 1997):

$$n_i(d_p, t) = N_i \, \delta(d_p - d_{p_i}) \quad (21)$$

where the particle number in each class (N_i) and d_{p_i} vary also with time (t) but its dependence has been omitted for notation simplicity.

Then, a general expression for the density function in the entire particle size domain can be written as:

$$n(d_p, t) = \sum_i n_i(d_p, t) = \sum_i N_i \delta(d_p - d_{p_i}) \quad (22)$$

3.1. Inlet/outlet terms

Although a function to represent the inlet density function flowrate can be used, in practice there are generally known discrete values $\dot{N}_{i_{in}}$ located on arbitrary sizes $\tilde{D}_p^{in}$, which are calculated from $\dot{n}_{in}$ as:

$$\dot{N}_{i_{in}} = \int_{D_{p_i}}^{D_{p_{i+1}}} \dot{n}_{in}(d_p, t) dd_p \quad (23)$$

On the other hand, the particle number flowrate leaving each class can be obtained by integrating the outlet density function flowrate as follows:

$$\dot{N}_{i_{out}} = \int_{D_{p_i}}^{D_{p_{i+1}}} \dot{n}_{out}(d_p, t) dd_p \quad (24)$$

For the particular case of a perfectly mixed system and non-classified discharge, Eq. (24) can be simplified to (Randolph and Larson, 1971):

$$\dot{N}_{i_{out}} = \int_{D_{p_i}}^{D_{p_{i+1}}} \frac{n(d_p, t)}{\tau} dd_p = \frac{N_i}{\tau} \quad (25)$$

where τ is the mean residence time, defined as the ratio between the total number of particles inside the system and the total outlet particle number flowrate.

3.2. Aggregation terms

By replacing Eq. (22) in (14), the following expression is obtained:

$$h^{A+}(d_p,t)=\frac{1}{2}\int_0^{\infty}\beta\left(x,(d_p^3-x^3)^{\frac{1}{3}}\right)\left[\sum_j N_j\delta(x-d_{p_j})\right]\times n\left((d_p^3-x^3)^{\frac{1}{3}}\right)\left[(d_p^3-x^3)^{-\frac{2}{3}}d_p^2\right]dx \tag{26}$$

Eq. (26) can be simplified to obtain:

$$h^{A+}(d_p,t)=\frac{1}{2}\sum_j\beta\left(d_{p_j},(d_p^3-d_{p_j}^3)^{\frac{1}{3}}\right)N_j n\left((d_p^3-d_{p_j}^3)^{\frac{1}{3}}\right)\times\left[(d_p^3-d_{p_j}^3)^{-\frac{2}{3}}d_p^2\right] \tag{27}$$

To calculate the particle number born by aggregation in class i, Eq. (27) is integrated with respect to d_p between two contiguous nodes as follows:

$$H_i^{A+}=\int_{D_{p_i}}^{D_{p_{i+1}}}h^{A+}(d_p,t)dd_p=\frac{1}{2}\int_{D_{p_i}}^{D_{p_{i+1}}}\sum_j\beta\left[d_{p_j},(d_p^3-d_{p_j}^3)^{\frac{1}{3}}\right]N_j n\left[(d_p^3-d_{p_j}^3)^{\frac{1}{3}}\right]dd_p \tag{28}$$

The density function in Eq. (28) can be written as:

$$n\left((d_p^3-d_{p_j}^3)^{\frac{1}{3}}\right)=\sum_k N_k\delta\left[(d_p^3-d_{p_j}^3)^{\frac{1}{3}}-d_{p_k}\right]=\sum_k N_k\delta\left(d_p-(d_{p_j}^3+d_{p_k}^3)^{\frac{1}{3}}\right)\left(\frac{d_{p_k}}{d_p}\right)^2 \tag{29}$$

By replacing Eq. (29) in (28):

$$H_i^{A+}=\frac{1}{2}\sum_j\sum_k\int_{D_{p_i}}^{D_{p_{i+1}}}\beta\left(d_{p_j},(d_p^3-d_{p_j}^3)^{\frac{1}{3}}\right)N_jN_k\delta\times\left(d_p-(d_{p_j}^3+d_{p_k}^3)^{\frac{1}{3}}\right)dd_p \tag{30}$$

Finally, Eq. (31) is obtained:

$$H_i^{A+}=\frac{1}{2}\sum_j\sum_{k/(j,k\to i)}\beta(d_{p_j},d_{p_k})N_jN_k \tag{31}$$

where the notation $k/(j,k\to i)$ means: all classes k such that aggregation between particles of classes j and k generate a particle of class i.

Following the development of Kumar et al. (2006), the average size of all newborn particles in class i is calculated by dividing the sectional moment μ_{q_i} of the total newborn particles by the total newborn particle number:

$$\bar{D}_{p_i}^{A}=\left[\frac{\sum_j\sum_{k/(j,k\to i)}\beta(d_{p_j},d_{p_k})N_jN_k(d_{p_j}^q+d_{p_k}^q)}{\sum_j\sum_{k/(j,k\to i)}\beta(d_{p_j},d_{p_k})N_jN_k}\right]^{\frac{1}{q}} \tag{32}$$

On the other hand, the term of particle death by aggregation is found by replacing Eq. (22) in (13) and integrating with respect to d_p between two contiguous nodes:

$$H_i^{A-}=\int_{D_{p_i}}^{D_{p_{i+1}}}h^{A-}(d_p,t)dd_p=N_i\sum_j\beta(d_{p_j},d_{p_k})N_j \tag{33}$$

3.3. Breakage terms

Regarding breakage, the following expression is obtained by replacing Eq. (22) in (18):

$$h^{B+}(d_p,t)=\int_{d_p}^{\infty}\nu(x)b(x)P(d_p,x)\sum_j N_j\delta(x-d_{p_j})dx=\sum_{d_{p_j}>d_p}\nu_jb_jP(d_p,d_{p_j})N_j \tag{34}$$

To calculate the particle number born by breakage, Eq. (34) is integrated with respect to d_p between two contiguous nodes as follows:

$$H_i^{B+}=\int_{D_{p_i}}^{D_{p_{i+1}}}h^{B+}(d_p,t)dd_p=\sum_j\nu_jb_jN_j\int_{D_{p_i}}^{D_{p_{i+1}}}P(d_p,d_{p_j})dd_p \tag{35}$$

Discrete values of $P(d_p,d_{p_j})$ are introduced through the following definition:

$$P_{ij}=\int_{D_{p_i}}^{D_{p_{i+1}}}P(d_p,d_{p_j})dd_p \tag{36}$$

Besides, particles of class i generated from the breakage of particles of class j are assigned to the average size that conserves the particle number and the sectional moment μ_{q_i}

$$\bar{D}_{p_{j\to i}}^{B}=\left[\frac{\int_{D_{p_{i+1}}}^{D_{p_i}}P(d_p,d_{p_j})d_p^q dd_p}{\int_{D_{p_{i+1}}}^{D_{p_i}}P(d_p,d_{p_j})dd_p}\right]^{\frac{1}{q}} \tag{37}$$

By replacing Eq. (36) in (35), the following expression for H_i^{B+} is obtained:

$$H_i^{B+}=\sum_{j>i}\nu_jb_jP_{ij}N_j \tag{38}$$

If a continuous function for P is available, $\nu_j=\nu(d_{p_j})$ can be computed from Eq. (19). On the other hand, if only discrete values of P are known, ν_j can be calculated from a μ_q conservation balance for each particle of size d_{p_j} that is breaking:

$$\nu_j=\frac{d_{p_j}^q}{\sum_k P_{kj}\bar{D}_{p_{j\to k}}^{B\,q}} \tag{39}$$

As for aggregation, the average size of all newborn particles by breakage in class i is calculated by dividing the sectional moment μ_{q_i} of the total newborn particles by the total newborn particle number:

$$\bar{D}_{p_i}^{B}=\left[\frac{\sum_{j>i}\nu_jb_jP_{ij}N_j\bar{D}_{p_{j\to i}}^{B\,q}}{\sum_{j>i}\nu_jb_jP_{ij}N_j}\right]^{\frac{1}{q}}=\left[\frac{\sum_{j>i}\nu_jb_jN_j\left[\int_{D_{p_i}}^{D_{p_{i+1}}}P(d_p,d_{p_j})d_p^q dd_p\right]}{\sum_{j>i}\nu_jb_jP_{ij}N_j}\right]^{\frac{1}{q}} \tag{40}$$

Taking into account Eqs. (16) and (22), the particle death term is written as:

$$H_i^{B-} = \int_{D_{p_i}}^{D_{p_{i+1}}} h^{B-}(d_p, t)dd_p = b_i N_i \tag{41}$$

3.4. Nucleation terms

The discretized nucleation term is obtained by integrating Eq. (20) with respect to d_p between contiguous nodes as follows:

$$\dot{N}_{nuc_i} = \int_{D_{p_i}}^{D_{p_{i+1}}} \dot{n}_{nuc} dd_p = B_{nuc_i} \tag{42}$$

$\dot{N}_{nuc_i}$ is the generation of particles of size $\bar{D}_{p_i}^N = d_{nuc}$ that appears for a given class i that satisfies $D_{p_i} < d_{nuc} < D_{p_{i+1}}$.

3.5. Growth term

As aforementioned and due to the accumulation, growth and attrition derivative terms, the PBE becomes a hyperbolic type equation (Kumar and Ramkrishna, 1997). The existence of growth/attrition requires a further analysis of the PBE. The property of the derivative of a product can be applied to the first two terms of the right-hand side of Eq. (1), and then the PBE can be rewritten as:

$$\frac{\partial n(d_p, t)}{\partial t} + [G(d_p) - A(d_p)]\frac{\partial n(d_p, t)}{\partial d_p} = \dot{n}_{in} - \dot{n}_{out} + h^{A+} - h^{A-} + h^{B+} - h^{B-} + \dot{n}_{nuc} - n(d_p, t)\frac{d}{dd_p}[G(d_p) - A(d_p)] \tag{43}$$

Hyperbolic equations have two important features. First, their solution can be interpreted as the propagation of the initial condition through the space coordinate (in this case, the internal coordinate) (LeVeque, 2002). Then, path lines (called *characteristics*) can be mapped in the (d_p, t) plane from every point of the initial condition, being $[G(d_p) - A(d_p)]$ the speed of propagation along the characteristics. Moreover, if the right-hand side of Eq. (43) is zero (i.e., $[G(d_p) - A(d_p)]$ is independent of the particle size and there are not aggregation, breakage, nucleation, inlet and outlet terms), the PBE solution can be regarded as a wave that propagates with a speed equal to $[G(d_p) - A(d_p)]$ (Strikwerda, 2004). Instead, if the right-hand side of Eq. (43) is not zero, an increase, decay or oscillations appear in the solution but the primary feature of the propagation of the solution along the characteristics is not altered (Ramkrishna, 2000).

Second, while Eq. (1) seems to have sense only if $n(d_p, t)$ is differentiable, the solution requires no differentiability of the initial or boundary conditions. Therefore, discontinuous solutions can be found (Strikwerda, 2004). In general, such discontinuities, which are a potential source of numerical instability, cannot often be accurately handled by numerical methods (Kumar, 2006).

Getting back to the original PBE formulation (Eq. (1)), the integration of the growth term between consecutive nodes, can be written as:

$$-\int_{D_{p_i}}^{D_{p_{i+1}}} \frac{\partial[G(d_p)n(d_p, t)]}{\partial d_p} dd_p = G(D_{p_i})n(D_{p_i}, t) - G(D_{p_{i+1}})n(D_{p_{i+1}}, t) \tag{44}$$

$G(D_{p_i})n(D_{p_i}, t)$ and $G(D_{p_{i+1}})n(D_{p_{i+1}}, t)$ represent the particle number flux that enter and exit each class i. To complete the discretization, it is necessary to express the above equation in terms of particle numbers rather than density functions. There are several methods to approximate $n(D_{p_i}, t)$ and $n(D_{p_{i+1}}, t)$ in terms of N_i (Hounslow et al., 1988; Ramkrishna, 2000; Kumar, 2006), and they strongly affect the accuracy of the discretization.

The use of Eq. (22) to compute particle number flux at nodes is not appropriate, since the $n(D_{p_i}, t)$ and $n(D_{p_{i+1}}, t)$ values are null. Instead, a number density function to spread the particles over the whole range of each class i is required. To this end, the following simple function is proposed to represent the number density in the discretized growth term:

$$n_i(d_p, t) = C_{1i}d_p + C_{2i} \tag{45}$$

where the parameters C_{1i} and C_{2i} are defined so that two sectional moments are satisfied: the 0th moment N_i and an arbitrary moment $\mu_{q_i} = N_i d_{p_i}^q$:

$$\int_{D_{p_i}}^{D_{p_{i+1}}} (C_{1i}d_p + C_{2i})dd_p = N_i \tag{46}$$

$$\int_{D_{p_i}}^{D_{p_{i+1}}} (C_{1i}d_p + C_{2i})d_p^q dd_p = N_i d_{p_i}^q \tag{47}$$

Integrating Eqs. (46) and (47) and solving for C_{1i} and C_{2i}:

$$C_{1i} = \frac{\frac{D_{p_{i+1}}^{q+1} - D_{p_i}^{q+1}}{D_{p_{i+1}} - D_{p_i}} - (q+1)d_{p_i}^q}{\frac{1}{2}(D_{p_{i+1}} + D_{p_i})(D_{p_{i+1}}^{q+1} - D_{p_i}^{q+1}) - \frac{q+1}{q+2}(D_{p_{i+1}}^{q+2} - D_{p_i}^{q+2})} N_i \tag{48}$$

$$C_{2i} = \frac{N_i - \frac{C_{1i}}{2}(D_{p_{i+1}}^2 - D_{p_i}^2)}{D_{p_{i+1}} - D_{p_i}} \tag{49}$$

This novel approach to represent the density number function at any particle size (Eqs. (45), (48) and (49)), satisfies exactly the total number of particles (or moment 0) and the generic moment μ_{q_i} (i.e., any other arbitrarily selected) at each class i (i.e., sectional moments) and consequently ensures the closure of both moments for the entire population.

Eqs. (48) and (49) can be replaced in (45) to obtain a continuous expression of $n(d_p, t)$ within each class i to be used in Eq. (44). $n(D_{p_i}, t)$ and $n(D_{p_{i+1}}, t)$ are:

$$n(D_{p_i}, t) = C_{1_{i-1}}D_{p_i} + C_{2_{i-1}} \tag{50}$$

$$n(D_{p_{i+1}}, t) = C_{1i}D_{p_{i+1}} + C_{2i} \tag{51}$$

As the particles that appear by growth into the ith class become from the size range $(i-1)$, the $n(D_{p_i}, t)$ is calculated using the C_1 and C_2 parameters corresponding to the previous class.

Although the integral between contiguous nodes of the linear function proposed in Eq. (45) has to be always positive, the linear function itself may numerically have negative values in a partial region of the interval $[D_{p_i}, D_{p_{i+1}}]$. In fact and as shown in Fig. 1, three possible cases of $n_i(d_p, t)$ vs. d_p can be found. According to Eq. (44), the number density function evaluated at the class nodes $n(D_{p_i}, t)$ and $n(D_{p_{i+1}}, t)$ cannot be negative for growth processes. Therefore $n(D_{p_i}, t)$ and $n(D_{p_{i+1}}, t)$ are assumed to be zero when they adopt negative values. This strategy has a physical basis: negative number density values adjacent to a class node can occur only when the particles are concentrated toward the other node. In other words, the mean diameter of the class that satisfies both selected moments is far away from the class node where n is negative. Taking into account this numerical approach, the discretized growth term is written as:

$$-\int_{D_{p_i}}^{D_{p_{i+1}}} \frac{\partial G(d_p)n(d_p, t)}{\partial d_p} dd_p = \alpha_{i-1}G(D_{p_i})(C_{1_{i-1}}D_{p_i} + C_{2_{i-1}}) - \alpha_i G(D_{p_{i+1}})(C_{1i}D_{p_{i+1}} + C_{2i}) \tag{52}$$

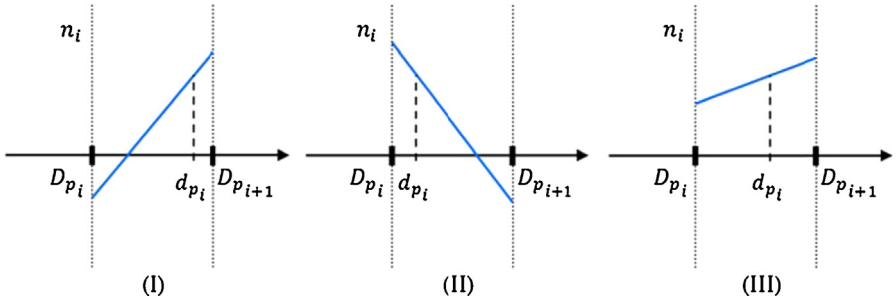

Fig. 1. Three possible cases for n_i in Eq. (44).

where:

$$\alpha_i = \begin{cases} 1 & \text{if}(C_{1i}D_{p_{i+1}} + C_{2i}) > 0 \\ 0 & \text{if}(C_{1i}D_{p_{i+1}} + C_{2i}) \leq 0 \end{cases} \tag{53}$$

According to Eq. (52), the particle number flux entering to each class i is computed based on information from class $(i-1)$. This strategy is consistent with the basic concept behind upwind methods, in which the positive convective speeds are written by means of a backward method (Pulliam and Zingg, 2014).

3.6. Attrition term

A discretized version of the attrition term can be derived following the same steps that those presented for the growth term. When the attrition term of Eq. (1) is integrated between consecutive nodes, the following discretized expression is obtained:

$$\int_{D_{p_i}}^{D_{p_{i+1}}} \frac{\partial[A(d_p)n(d_p,t)]}{\partial d_p} dd_p = A(D_{p_{i+1}})n(D_{p_{i+1}},t) - A(D_{p_i})n(D_{p_i},t) \tag{54}$$

$A(D_{p_{i+1}})n(D_{p_{i+1}},t)$ and $A(D_{p_i})n(D_{p_i},t)$ represent the particle number fluxes that enter and exit each class i. As in growth, Eq. (45) is used to represent $n_i(d_p,t)$, with C_{1i} and C_{2i} calculated from Eqs. (48) and (49), respectively. Because in attrition the particle number flux is negative along the d_p direction, $n(D_{p_i},t)$ and $n(D_{p_{i+1}},t)$ are approximated as:

$$n(D_{p_i},t) = C_{1i}D_{p_i} + C_{2i} \tag{55}$$

$$n(D_{p_{i+1}},t) = C_{1_{i+1}}D_{p_{i+1}} + C_{2_{i+1}} \tag{56}$$

Finally, the discretized attrition term is written as:

$$\int_{D_{p_i}}^{D_{p_{i+1}}} \frac{\partial A(d_p)n(d_p,t)}{\partial d_p} dd_p = \gamma_{i+1}A(D_{p_{i+1}})(C_{1_{i+1}}D_{p_{i+1}} + C_{2_{i+1}}) - \gamma_i A(D_{p_i})(C_{1i}D_{p_i} + C_{2i}) \tag{57}$$

where:

$$\gamma_i = \begin{cases} 1 & \text{si}(C_{1i}D_{p_i} + C_{2i}) > 0 \\ 0 & \text{si}(C_{1i}D_{p_i} + C_{2i}) \leq 0 \end{cases} \tag{58}$$

In Eq. (57), the particle number flux entering to each class i is computed with the information of class $(i+1)$. Similarly to growth, Eq. (57) is an upwind method, in which the negative convective speeds are written by means of an upward scheme (Pulliam and Zingg, 2014).

3.7. Discretized PBE

According to the discretization of all the PBE terms above detailed, Eq. (1) becomes:

$$\begin{aligned} \frac{dN_i}{dt} &= \alpha_{i-1}G(D_{p_i})(C_{1_{i-1}}D_{p_i} + C_{2_{i-1}}) - \alpha_i G(D_{p_{i+1}})(C_{1i}D_{p_{i+1}} + C_{2i}) \\ &+ \gamma_{i+1}A(D_{p_{i+1}})(C_{1_{i+1}}D_{p_{i+1}} + C_{2_{i+1}}) - \gamma_i A(D_{p_i})(C_{1i}D_{p_i} + C_{2i}) \\ &+ \dot{N}_{i_{in}} - \dot{N}_{i_{out}} + H_i^{A+} - H_i^{A-} + H_i^{B+} - H_i^{B-} + \dot{N}_{i_{nuc}} \end{aligned} \tag{59}$$

Eq. (59) is complemented by Eqs. (53), (58), (48), (49), (23), (24), (31), (33), (38), (41) and (42) for the evaluation of α_i, γ_i, C_{1i}, C_{2i}, $\dot{N}_{i_{in}}$, $\dot{N}_{i_{out}}$, H_i^{A+}, H_i^{A-}, H_i^{B+}, H_i^{B-} and $\dot{N}_{i_{nuc}}$, respectively. Since many of these variables are dependent on d_{p_i}, an extra equation is still necessary.

The mean size that satisfies the sectional population moments 0 and $\mu_{q_i x}$ in each class, d_{p_i}, is given by:

$$d_{p_i} = \left(\frac{\mu_{q_i}}{N_i}\right)^{\frac{1}{q}} \tag{60}$$

Therefore, its rate of change becomes:

$$\frac{dd_{p_i}}{dt} = \frac{d_{p_i}^{1-q}}{qN_i}\left(\frac{d\mu_{q_i}}{dt} - d_{p_i}^q \frac{dN_i}{dt}\right) \tag{61}$$

The μ_{q_i} change rate is obtained by multiplying Eq. (1) by d_p^q and integrating with respect to d_p between D_{p_i} and $D_{p_{i+1}}$:

$$\begin{aligned} \frac{d\mu_{q_i}}{dt} &= -\int_{D_{p_i}}^{D_{p_{i+1}}} \frac{\partial}{\partial d_p}[G(d_p)n(d_p,t)]d_p^q dd_p \\ &+ \int_{D_{p_i}}^{D_{p_{i+1}}} \frac{\partial}{\partial d_p}[A(d_p)n(d_p,t)]d_p^q dd_p \\ &+ \int_{D_{p_i}}^{D_{p_{i+1}}} (\dot{n}_{in} - \dot{n}_{out} + h^{A+} - h^{A-} + h^{B+} - h^{B-} + \dot{n}_{nuc})d_p^q dd_p \end{aligned} \tag{62}$$

The first term of the right-hand side in Eq. (62) is integrated by parts as follows:

$$\begin{aligned} &-\int_{D_{p_i}}^{D_{p_{i+1}}} \frac{\partial}{\partial d_p}[G(d_p)n(d_p,t)]d_p^q dd_p \\ &= q\int_{D_{p_i}}^{D_{p_{i+1}}} G(d_p)n(d_p,t)d_p^{q-1}dd_p - G(d_p)n(d_p,t)d_p^q\Big|_{D_{p_i}}^{D_{p_{i+1}}} \end{aligned} \tag{63}$$

The relationships given by Eqs. (22) and (45) are used in the first and second terms of the right-hand side in Eq. (63) to obtain:

$$-\int_{D_{p_i}}^{D_{p_{i+1}}} \frac{\partial}{\partial d_p}[G(d_p)n(d_p,t)]d_p^q dd_p$$
$$= qG(d_{p_i})N_i d_{p_i}^{q-1} + \alpha_{i-1}G(D_{p_i})(C_{1_{i-1}}D_{p_i} + C_{2_{i-1}})D_{p_i}^q$$
$$- \alpha_i G(D_{p_{i+1}})(C_{1i}D_{p_{i+1}} + C_{2i})D_{p_{i+1}}^q \quad (64)$$

Similarly to growth, the attrition term in Eq. (62) becomes:

$$\int_{D_{p_i}}^{D_{p_{i+1}}} \frac{\partial}{\partial d_p}[A(d_p)n(d_p,t)]d_p^q dd_p$$
$$= -qA(d_{p_i})N_i d_{p_i}^{q-1} + \gamma_{i+1}A(D_{p_{i+1}})(C_{1_{i+1}}D_{p_{i+1}} + C_{2_{i+1}})D_{p_{i+1}}^q$$
$$- \gamma_i A(D_{p_i})(C_1 D_{p_i} + C_{2i})D_{p_i}^q \quad (65)$$

The integral of the last term in Eq. (62) can be solved by using Dirac functions to represent the density functions:

$$\int_{D_{p_i}}^{D_{p_{i+1}}} (\dot{n}_{in} - \dot{n}_{out} + h^{A+} - h^{A-} + h^{B+} - h^{B-} + \dot{n}_{nuc})d_p^q dd_p$$
$$= \int_{D_{p_i}}^{D_{p_{i+1}}} \dot{N}_{i_{in}}\delta(d_p - \bar{D}_p^{in})d_p^q dd_p + \int_{D_{p_i}}^{\infty} H_i^{A+}\delta(d_p - \bar{D}_{p\,i}^{A})d_p^q dd_p$$
$$+ \int_{D_{p_i}}^{D_{p_{i+1}}} H_i^{B+}\delta(d_p - \bar{D}_{p\,i}^{B})d_p^q dd_p + \int_{D_{p_i}}^{\infty} \dot{N}_{i_{nuc}}\delta(d_p - \bar{D}_{p\,i}^{N})d_p^q dd_p$$
$$- \int_{D_{p_i}}^{D_{p_{i+1}}} (\dot{N}_{i_{out}} + H_i^{A-} + H_i^{B-})\delta(d_p - d_{p_i})d_p^q dd_p \quad (66)$$

Therefore, the balance for μ_{q_i} becomes:

$$\frac{d\mu_{q_i}}{dt} = q[G(d_{p_i}) - A(d_{p_i})]N_i d_{p_i}^{q-1} + \alpha_{i-1}G(D_{p_i})(C_{1_{i-1}}D_{p_i} + C_{2_{i-1}})D_{p_i}^q$$
$$- \alpha_i G(D_{p_{i+1}})(C_{1i}D_{p_{i+1}} + C_{2i})D_{p_{i+1}}^q + \gamma_{i+1}A(D_{p_{i+1}})$$
$$\times (C_{1_{i+1}}D_{p_{i+1}} + C_{2_{i+1}})D_{p_{i+1}}^q - \gamma_i A(D_{p_i})(C_{1i}D_{p_i} + C_{2_i})D_{p_i}^q$$
$$+ \dot{N}_{i_{in}}\bar{D}_p^{in\,q} + H_i^{A+}\bar{D}_{p\,i}^{A\,q} + H_i^{B+}\bar{D}_{p\,i}^{B\,q} + \dot{N}_{i_{nuc}}\bar{D}_{p\,i}^{N\,q}$$
$$- (\dot{N}_{i_{out}} + H_i^{A-} + H_i^{B-})d_{p_i}^q \quad (67)$$

By replacing Eqs. (59) and (67) in (61), the following equation for d_{p_i} is obtained:

$$\frac{dd_{p_i}}{dt} = G(d_{p_i}) - A(d_{p_i}) + \frac{\alpha_{i-1}d_{p_i}^{1-q}}{qN_i}G(D_{p_i})(C_{1_{i-1}}D_{p_i} + C_{2_{i-1}})(D_{p_i}^q - d_{p_i}^q)$$
$$- \frac{\alpha_i d_{p_i}^{1-q}}{qN_i}G(D_{p_{i+1}})(C_{1i}D_{p_{i+1}} + C_{2_i})(D_{p_{i+1}}^q - d_{p_i}^q)$$
$$+ \frac{\gamma_{i+1}d_{p_i}^{1-q}}{qN_i}A(D_{p_{i+1}})(C_{1_{i+1}}D_{p_{i+1}} + C_{2_{i+1}})(D_{p_{i+1}}^q - d_{p_i}^q)$$
$$- \frac{\gamma_i d_{p_i}^{1-q}}{qN_i}A(D_{p_i})(C_{1i}D_{p_i} + C_{2i})(D_{p_i}^q - d_{p_i}^q)$$
$$+ \frac{d_{p_i}^{1-q}}{qN_i}[\dot{N}_{i_{in}}(\bar{D}_{p_i}^{in\,q} - d_{p_i}^q) + H_i^{A+}(\bar{D}_{p\,i}^{A\,q} - d_{p_i}^q)$$
$$+ H_i^{B+}(\bar{D}_{p\,i}^{B\,q} - d_{p_i}^q) + \dot{N}_{i_{nuc}}(\bar{D}_{p\,i}^{N\,q} - d_{p_i}^q)] \quad (68)$$

Eq. (59) must be solved together with Eq. (68) for each class i. Eq. (68) predicts the change of the location of the representative particle size d_{p_i}. In Eq. (68), $[G(d_{p_i}) - A(d_{p_i})]$ represents the convective movement of the particles within each class, and the following four terms describe the passage of the particles through the class interfaces due to growth and attrition. The inlet stream and aggregation, breakage and nucleation mechanisms modify the d_{p_i} value by means of the last term of Eq. (68). Is important to note that, if only aggregation and/or rupture occur, the method becomes the moving pivot technique presented by Kumar and Ramkrishna (1996b). The new contribution is the discretization performed for the growth and attrition terms, in which a linear approximation for the density function within each class is considered to estimate the convective fluxes at the cell boundaries. On the other hand, the fluxes are split in positive and negative contributions (i.e., growth or attrition); the flux at each class boundary is calculated once the upwind direction is available. Then, the proposed strategy corresponds to a flux-vector splitting method (LeVeque, 2002). Moreover, the need to apply a physical limitation to the particle flux when $G < 0$ or $A < 0$ by simply setting the unphysical flux to zero restricts the numerical diffusion.

The second original contribution is the coupling between the moving pivot technique of Kumar and Ramkrishna and the discretization performed for growth and attrition terms. The usage of a linear density function consistent with the same two population moments conserved by the pivot moving discretization allows to preserve the sectional and global population moments even as all the size change mechanisms occur simultaneously.

The use of a representative particle diameter for each class that is continuously updated avoids the need of reassignment of new born particles to existing predefined sizes, as the fixed pivot technique of Kumar and Ramkrishna (1996a) or the cell average method of Kumar et al. (1997). Although in the literature is recognized that this feature gives difficulties to solve the resulting set of ordinary differential equations requiring more computation time and resulting in a system of stiff differential equations (Kumar et al., 2006; Nopens and Vanrolleghem, 2006), the predictions of the moving pivot technique show superior predictions.

4. A simple example to illustrate the growth term discretization

As it is mentioned in Section 3.7, the proposed strategy for describing the four first terms of the right-hand side in Eq. (59) is an upwind method which uses a decomposition or splitting of the fluxes into terms with positive and negative convective speeds so that appropriate differences schemes can be chosen for each. The application of physical limitations (through Eqs. (53) and (58)) to the particle fluxes by simply setting the unphysical values to zero is the reason for the reduction in numerical diffusion.

To illustrate the behavior of the growth term discretization, a simple numerical example with a constant growth rate $G = 0.001$ m/s is solved and analyzed for a coating batch process. For the numerical simulation, an arithmetic grid with $D_{p_1} = 0$ and a class width equal to 0.001 m is used. The initial population consists of 100 particles located in class 2 (i.e., particle sizes between 0.001 and 0.002 m), as it can be seen in Fig. 2a. Besides, it is assumed that the representative diameter of the initial population is 0.0015 m (arithmetic mean size for class 2). The numerical method is applied to preserve the moments 0 and 3 (i.e., $q = 3$).

Fig. 2b shows, for $t = 0$, the linear number density function n_i for the only class where particles exist, defined by Eq. (45), and the representative diameter that conserves the chosen population moments. As the initial representative diameter is the midpoint of the class length and sectional moments 0 and 3 are conserved, C_{1i}

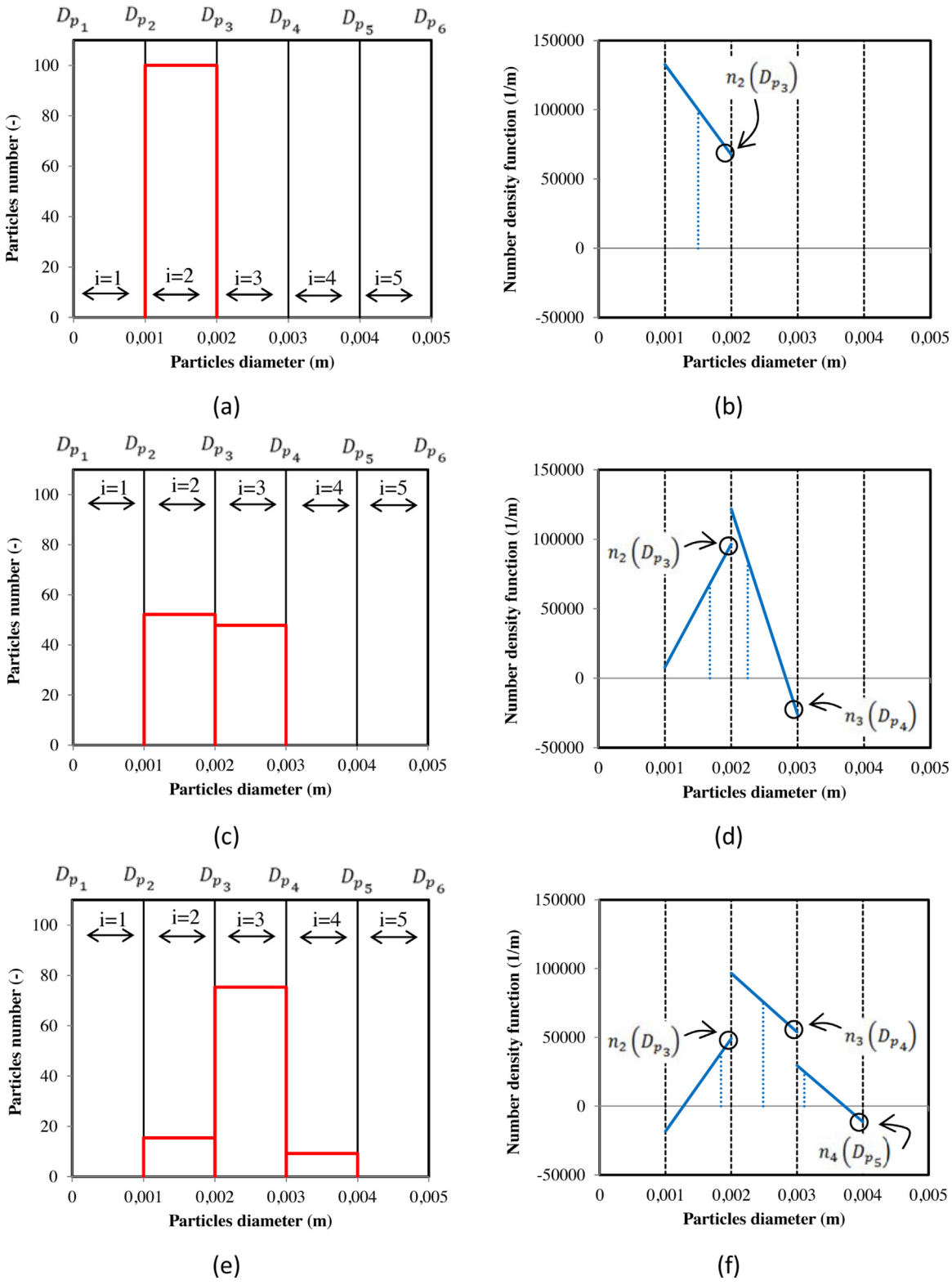

Fig. 2. Example to illustrate the growth term discretization procedure (Section 4).

and C_{2i} are such that n_2 decreases (see Eq. (45)). The particle number flux that exit from class 2 and enter to class 3 due to growth depends on the value of $n_2 = (C_{12}D_{p3} + C_{22})$ (see Eq. (52)). Since this value is positive, there is a particle convective flux toward class 3.

For $t = 0.5$ s, Fig. 2c shows the calculated PSD expressed as particle number. As it can be seen, 52 particles are still in class 2, while 48 particles grew to sizes within class 3. In addition, the simulation results indicate that no particles grew enough to be within class 4. These results are consistent with Fig. 2d, in which the corresponding number density function is presented. The representative diameter d_{p3} is equal to 0.00225 m, which means that N_3 is far from the interface between classes 3 and 4 (i.e., $D_{p4} = 0.003$ m).

Then, $n_3 = (C_{13}D_{p4} + C_{23})$ is negative and the particle convective flux toward class 4 is null.

Fig. 2e shows the calculated PSD expressed as particle number for $t = 1$ s. At this time, the PSD is distributed over three classes ($i = 2$–4). Classes 2 and 3 have 16 and 75 particles, respectively, while 9 particles grew enough to be within class 4. According to Fig. 2f, $n_3 = (C_{13}D_{p4} + C_{23})$ is positive, indicating that the particle convective flux at the interface between classes 3 and 4 must be positive. On the other hand, particles in class 4 have a representative size ($d_{p4} = 0.00311$ m) close to the lowest boundary of class 4. Then $n_4 = (C_{14}D_{p5} + C_{24})$ is negative and the particle convective flux from class 4 to class 5 is null.

5. Accuracy of the proposed method

The proposed numerical method can be applied to solve all the combinations of size change mechanisms in perfectly mixed batch or unsteady/steady-state continuous processes. In this section, different examples, for which analytical solutions are available, are considered to validate the numerical technique. PBEs for single and multiple simultaneous size change mechanisms are included to verify the accuracy of the numerical method. Specifically, the eight study cases shown in Table 1 are analyzed.

For all these cases, it is considered that particles are spherical and that the population moments 0 and 3 are conserved. For the examples corresponding to continuous system (cases 1, 4 and 7), the mean diameter of each class in the inlet flow rate is calculated by conserving the sectional moments 0 and 3:

$$\tilde{D}_{p_i}^{in} = \left(\frac{\int_{D_{p_{i+1}}}^{D_{p_i}} \dot{n}_{in} d_p^3 dd_p}{\int_{D_{p_{i+1}}}^{D_{p_i}} \dot{n}_{in} dd_p} \right)^{\frac{1}{3}} \tag{69}$$

For each case, the prediction of these moments is evaluated by calculating the relative difference between the population moments obtained from the density function (by means of Eq. (4)) and the macroscopic balances (which are below presented for each case):

$$\frac{\mu_0|_{PBE} - \mu_0|_{balance}}{\mu_0|_{balance}} = \frac{N|_{PBE} - N|_{balance}}{N|_{balance}} \tag{70}$$

$$\frac{\mu_3|_{PBE} - \mu_3|_{balance}}{\mu_3|_{balance}} = \frac{V|_{PBE} - V|_{balance}}{V|_{balance}} \tag{71}$$

The results of this section are shown in Figs. 3–10. The PSDs are plotted as number density function vs. particle diameter. To this

Table 1
Study cases to evaluate the accuracy of the numerical method.

Case	Operation mode	Size change mechanisms	Size change kinetics	Simulation parameters	Maximum error	
					Moment 0	Moment 3
1	Continuous, steady state	Aggregation	Constant aggregation rate	$Q_{in} = 0.02\ m^3/s$ $V_0 = 4\ m^3$	0.03%	0.03%
2	Batch	Growth	Power law growth rate	$V_0 = 0.02\ m^3$ $N_0 = 62{,}809$ $Q_{growth} = 3 \times 10^{-4}\ m^3/s$ $\mu_0 = 0.008$ m $\sigma_0 = 0.002$ m $t = 100$ s	0.01%	0.01%
3	Batch	Growth + Attrition	Linear increase of the net growth rate with the particle diameter, for particles different than a critical size	$N_0 = 5.40 \times 10^4$ $G_0' = 4 \times 10^{-5}$ m/s $d_{p\,crit} = 0.008$ m $\lambda = 0.007$ m $\mu_0 = 0.008$ m	0.001%	0.2%
4	Continuous, steady state	Breakage	Breakage rate proportional to particle size. Breakage probability function: each broken particle generates four fragments	$d_{pin} = 0.0005$ m	0.5%	2×10^{-5}%
5	Batch	Growth + Aggregation	Constant aggregation rate. Growth rate proportional to particle volume	$d_0 = 0.0156$ m $t = 100$ s	0.1%	1%
6	Batch	Aggregation + Breakage	Constant aggregation rate. Breakage rate proportional to particle volume Breakage probability function: each broken particle generates two fragments	$t = 100$ s	0.26%	0.003%
7	Continuous, steady state	Attrition	Constant attrition rate	$d_{p_0} = 0.001$ m $Q_{in} = 0.001\ m^3/s$ $\tau = 10$ s	0.5%	1%
8	Batch	Growth + Nucleation	Growth rate independent of particle size Constant nucleation rate	$V_0 = 0.01\ m^3$ $G = 2 \times 10^{-6}$ m/s $d_0 = 0.001$ m $d_{nuc} = \bar{D}_{p1}$	0.5%	1%

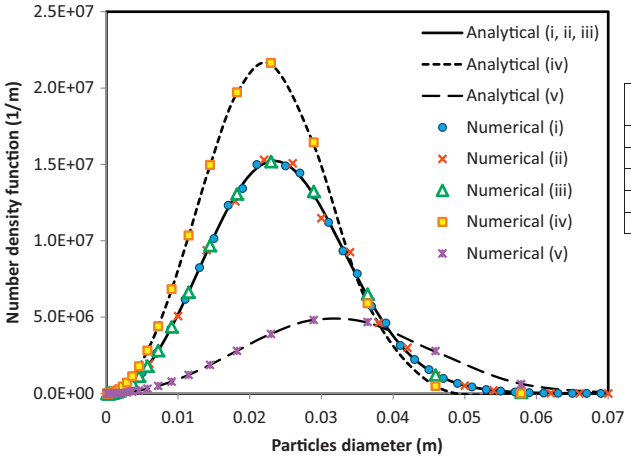

Test	Grid	d_0 (m)	β (s-1)
i	A	0.025	1×10^{-8}
ii	B	0.025	1×10^{-8}
iii	C	0.025	1×10^{-8}
iv	C	0.025	1×10^{-9}
v	C	0.05	1×10^{-8}

Fig. 3. Comparison of analytical and numerical PSDs for Case 1 (Grid A: arithmetic grid, $D_{p1} = 0$ mm, 34 classes, class width = 0.002 m; Grid B: arithmetic grid, $D_{p1} = 0$ mm, 17 classes, class width = 0.004 m; Grid C: geometric grid, $D_{p1} = 1 \times 10^{-4}$ m, 30 classes, $r = 2^{1/3}$).

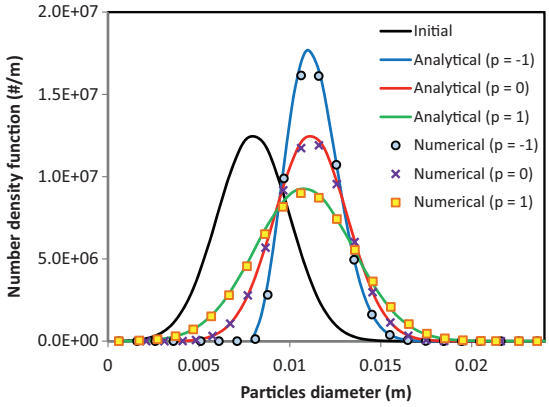

Fig. 4. Comparison of analytical and numerical PSDs for Case 2 (arithmetic grid, $D_{p1} = 1 \times 10^{-4}$ m, 30 classes, class width = 0.001 m).

end, the number of particles in each class (N_i), which is calculated by the numerical method (Eq. (59)), is converted, to the discrete number density function n_i by dividing each N_i by the class width ($D_{p_{i+1}} - D_{p_i}$).

5.1. Case 1

This problem was previously studied by Hounslow (1990). The PBE for this case becomes:

$$\dot{n}_{in} - \dot{n}_{out} + h^{A+} - h^{A-} = 0 \tag{72}$$

The inlet PSD is given as:

$$\dot{n}_{in} = \dot{N}_{in} \frac{3d_p^2}{d_0^3} e^{-\left(\frac{d_p}{d_{nv}}\right)^3} \tag{73}$$

where d_{nv} is the number–volume mean diameter of the inlet PSD. The aggregation kernel is assumed to be constant. For a perfectly mixed system, the normalized outlet PSD is equal to the one inside the system. Then, the flow of particles exiting the unit can be formulated as:

$$\dot{n}_{out} = \frac{n(d_p)}{\tau} \tag{74}$$

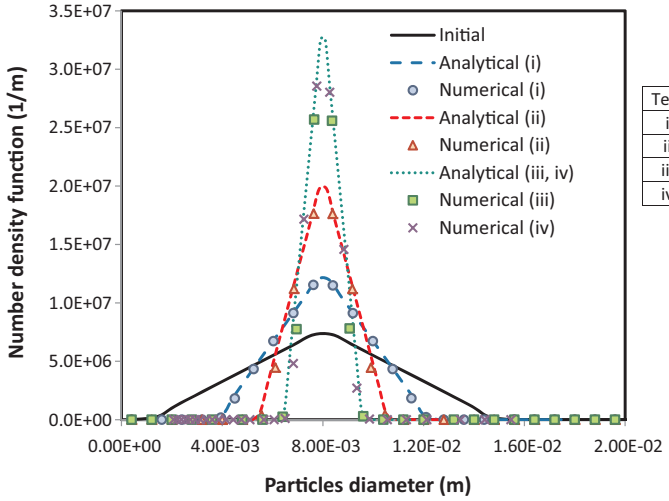

Test	Grid	t (s)
i	A	100
ii	A	200
iii	A	300
iv	B	300

Fig. 5. Comparison of analytical and numerical PSDs for Case 3 (Grid A: arithmetic grid, $D_{p1} = 0$ m, 30 classes, class width = 0.0008 m; Grid B: geometric grid, $D_{p1} = 0.002$ m, 30 classes, $r = 2 \times 10^{1/10}$).

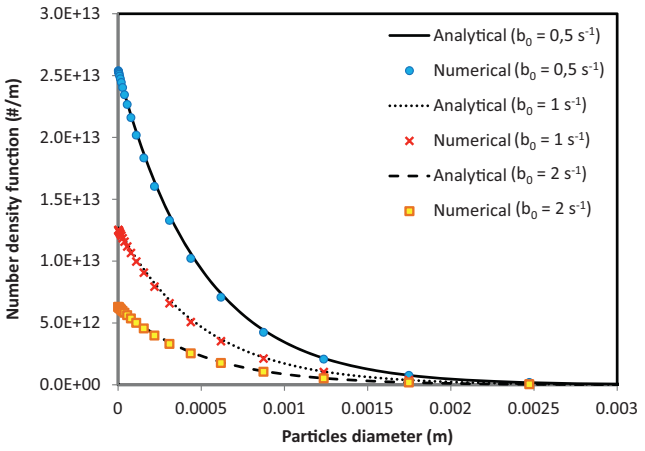

Fig. 6. Comparison of analytical and numerical PSDs for Case 4 (geometric grid, $D_{p1} = 1 \times 10^{-6}$ m, 30 classes, $r = 2^{1/2}$).

For the inlet PSD and the conditions above-mentioned, the analytical solution is given by (Hounslow, 1990):

$$n(d_p) = \dot{N}_{in}\tau \frac{3d_p^2}{d_0^3} \frac{I_0\left[\frac{-T}{1+2T}\left(\frac{d_p}{d_0}\right)^3\right] + I_1\left[\frac{-T}{1+2T}\left(\frac{d_p}{d_0}\right)^3\right]}{e^{\frac{(1+T)}{1+2T}\left(\frac{d_p}{d_0}\right)^3}\sqrt{1+2T}} \tag{75}$$

where T is a dimensionless time defined as:

$$T = \beta \dot{N}_{in} \tau^2 \tag{76}$$

I_0 and I_1 are the modified Bessel function of the first kind of order zero and one, respectively:

$$I_0\left(\left(\frac{d_p}{d_0}\right)^3\right) = \sum_{k=0}^{\infty} \frac{\left[\frac{1}{4}\left(\frac{d_p}{d_0}\right)^3\right]^k}{k!\,\Gamma(k+1)} \tag{77}$$

$$I_1\left(\left(\frac{d_p}{d_0}\right)^3\right) = \frac{d_p}{2d_0} \sum_{k=0}^{\infty} \frac{\left[\frac{1}{4}\left(\frac{d_p}{d_0}\right)^3\right]^k}{k!\,\Gamma(k+2)} \tag{78}$$

Γ is the gamma function. To calculate the total particle number N within the system, Eq. (75) should be integrated with respect to d_p between zero and infinity. Alternatively, N can be obtained by solving Eq. (5) for $j = 0$. By doing this, Eq. (5) becomes:

$$\dot{N}_{in} - \frac{N}{\tau} + \frac{\beta}{2}N^2 - \beta N^2 = 0 \tag{79}$$

Then, N is described by the following expression:

$$N\big|_{balance} = \frac{-1 + \sqrt{1 + 2\tau^2 \beta \dot{N}_{in}}}{\tau\beta} \tag{80}$$

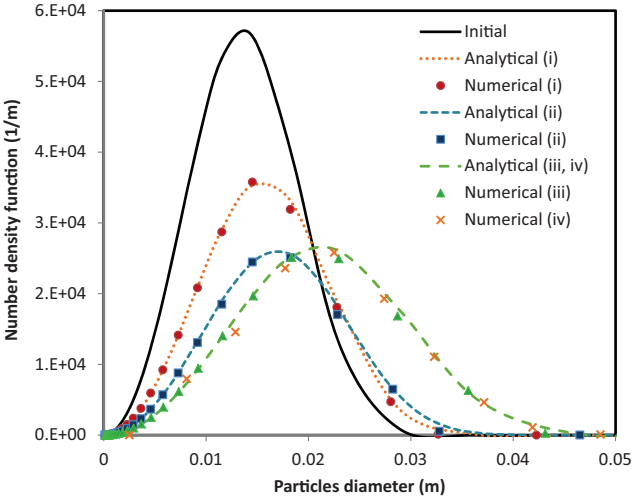

Test	Grid	G_0'' (s^{-1})	β (s^{-1})
i	A	1×10^{-3}	1×10^{-5}
ii	A	1×10^{-2}	2×10^{-5}
iii	A	1×10^{-2}	1×10^{-5}
iv	B	1×10^{-2}	1×10^{-5}

Fig. 7. Comparison of analytical and numerical PSDs for Case 5 (Grid A: geometric grid, $D_{p1} = 0.0001$ m, 30 classes, $r = 2^{1/3}$; Grid B: arithmetic grid, $D_{p1} = 0$ m, 10 classes, class width = 0.005 m).

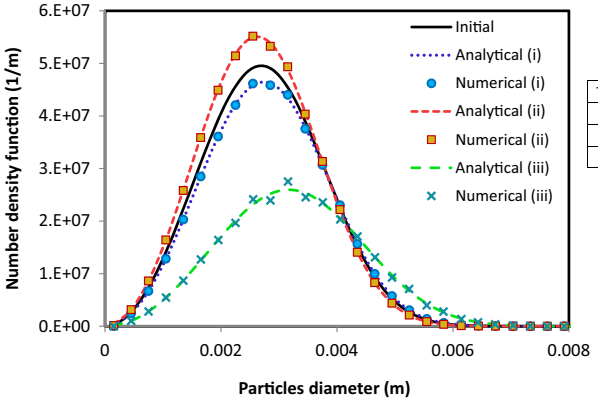

Test	β (s^{-1})	b_0'' ($m^{-3}s^{-1}$)
i	1×10^{-8}	1×10^{4}
ii	1×10^{-8}	1×10^{5}
iii	1×10^{-7}	1×10^{4}

Fig. 8. Comparison of analytical and numerical PSDs for Case 6 (arithmetic grid, $D_{p1} = 0$ m, 30 classes, class width = 3×10^{-4} m).

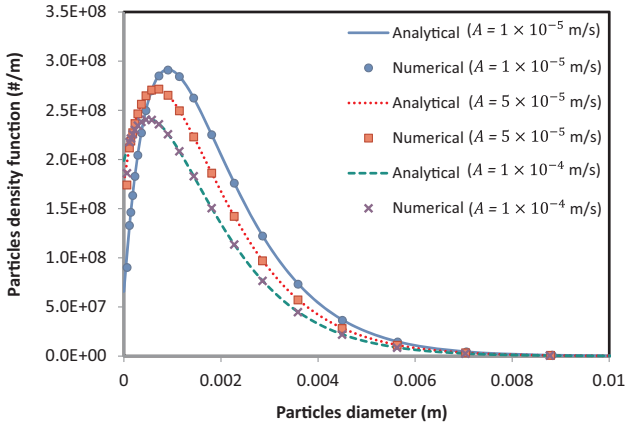

Fig. 9. Comparison of analytical and numerical PSDs for Case 7 (Grid: $D_{p1} = 0$, $D_{p2} = 1 \times 10^{-4}$ m, $D_{pk} = D_{pk-1} 2^{1/3}$ for $k = 3$–31).

Since the system is under a steady-state operation and only aggregation occurs, the total particle volume remains constant. Then V, obtained from the macroscopic balance, becomes:

$$V\big|_{balance} = Q_{out}\tau = Q_{in}\tau \tag{81}$$

In Fig. 3, the discrete number density values obtained by using the proposed numerical method are compared with the analytical solution for five different tests. The simulation conditions and parameters used in the calculations are presented in Table 1. The results show that the numerical method provides very accurate solutions for both arithmetic and geometric grids and for different grid coarseness and number of classes. Since the only size change mechanism is aggregation, the numerical method matches the moving pivot technique of Kumar and Ramkrishna (1996b). Then it is expected that moments 0 and 3 are well conserved. In fact, according to Table 1 the numerical errors lower than 0.03% for both population moments.

5.2. Case 2

For a perfectly mixed batch system and pure growth, the PBE (Eq. (1)) becomes:

$$\frac{\partial n(d_p,t)}{\partial t} = -\frac{\partial}{\partial d_p}[G(d_p)n(d_p,t)] \tag{82}$$

In order to find an analytical solution, a general power-law model for the particle growth rate is assumed (Alexopolous et al., 2005):

$$G(d_p) = G_0 d_p^p \tag{83}$$

where G_0 and p are particle growth rate constants. For spherical particles, Eq. (9) becomes:

$$G_0 = \frac{2Q_{growth}}{\pi\mu_{2+p}} \tag{84}$$

Eq. (84) indicates that G_0 and p cannot be independently chosen for a given Q_{growth}. Furthermore, if Q_{growth} and μ_{2+p} are a function of t, G_0 is also time dependent.

The analytical solution of Eq. (82) for the above-mentioned assumption can be derived by using the Method of Characteristics (Kumar and Ramkrishna, 1997; Ramkrishna, 2000). By applying this technique, $n(d_p)$ is obtained as a parameterized equation, i.e., as a set of coordinates (n, d_p) which are a function of t:

$$n(t) = \begin{cases} n_0(d_{p_0})\left[1 + \dfrac{(1-q)}{d_{p_0}^{1-p}}\displaystyle\int_0^t G_0 dt\right]^{-\frac{p}{1-p}} & p \neq 1 \\ n_0(d_{p_0})e^{-\int_0^t G_0 dt} & p = 1 \end{cases} \tag{85}$$

$$d_p(t) = \begin{cases} \left[d_{p_0}^{1-p} + (1-p)\displaystyle\int_0^t G_0 dt\right]^{\frac{1}{1-p}} & p \neq 1 \\ d_{p_0} e^{\int_0^t G_0 dt} & p = 1 \end{cases} \tag{86}$$

$n_0(d_{p_0})$ is the initial PSD which provides the initial values $n(0) = n_0$ and $d_p(0) = d_{p_0}$. Eqs. (87) and (88) describe the evolution of $n(t)$ and $d_p(t)$ for every point of the initial PSD.

To evaluate the accuracy of the proposed numerical method, the initial PSD is supposed to be Gaussian:

$$n_0(d_{p_0}) = \frac{N_0}{\sqrt{2\pi}\sigma_0} e^{-\frac{1}{2}\left(\frac{d_{p_0}-\mu_0}{\sigma_0}\right)^2} \tag{87}$$

where μ_0 and σ_0 are the arithmetic mean diameter and standard deviation for n_0.

For Case 2 only growth occurs in a batch system, then N remains equal to its initial value N_0.

$$N\big|_{balance} = N_0 \tag{88}$$

On the other hand, the total particle volume V increases due to Q_{growth}. Then, the total volume balance becomes:

$$\frac{dV}{dt} = Q_{growth} \tag{89}$$

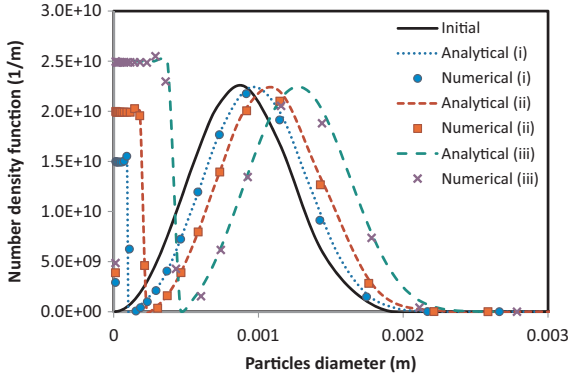

Test	B (s^{-1})	t (s)
i	30000	50
ii	40000	100
iii	50000	200

Fig. 10. Comparison of analytical and numerical PSDs for Case 8 (geometric grid, 30 classes, $D_{p1} = 1 \times 10^{-5}$ m, $r = 2^{1/3}$).

By considering a constant Q_{growth} value:

$$V\big|_{balance} = V_0 + Q_{growth}t \tag{90}$$

Table 1 shows the parameter values and discretization grid used in the simulations. Fig. 4 shows that the numerical method is able to accurately calculate the PSD for the three potential growth laws, even for test (i) that exhibits the sharpest PSD. As indicated in Table 1, errors in the predictions of moments 0 and 3 are lower than 0.01%. As it can be seen in Fig. 4, the use of the proposed discretization technique avoids the presence of non-physical oscillations in the number density function for low sizes, which is commonly observed when the PBE is discretized by finite differences.

5.3. Case 3

To predict the PSD in perfectly mixed batch operation where growth and attrition occur simultaneously, the PBE is given by:

$$\frac{\partial n(d_p,t)}{\partial t} + \frac{\partial}{\partial d_p}[(G(d_p) - A(d_p))n(d_p,t)] = 0 \tag{91}$$

To evaluate the method accuracy to predict narrow PSDs, the following linear equation is chosen to represent the net growth rate ($G(d_p) - A(d_p)$):

$$G(d_p) - A(d_p) = G_0'\left(1 - \frac{d_p}{d_{p_{crit}}}\right) \tag{92}$$

G_0' is the growth rate for punctual particles (i.e., $d_p \to 0$) and $d_{p_{crit}}$ is a critical diameter which enables or disables the growth or attrition mechanism. Therefore, particles with diameters less than $d_{p_{crit}}$ increase in size while those particles larger than $d_{p_{crit}}$ tend to shrink. According to Eq. (92), the growth and attrition rate can be written as:

$$G(d_p) = \begin{cases} G_0'\left(1 - \dfrac{d_p}{d_{p_{crit}}}\right) & \text{if } d_p < d_{p_{crit}} \\ 0 & \text{if } d_p \geq d_{p_{crit}} \end{cases} \tag{93}$$

$$A(d_p) = \begin{cases} 0 & \text{if } d_p < d_{p_{crit}} \\ -G_0'\left(1 - \dfrac{d_p}{d_{p_{crit}}}\right) & \text{if } d_p \geq d_{p_{crit}} \end{cases} \tag{94}$$

The selected initial PSD is described by means of a triangular pulse function centered in μ_0 with a 2λ width; thus, the pulse is limited by $(\mu_0 - \lambda)$ and $(\mu_0 + \lambda)$:

$$n_0(d_p) = N_0 \begin{cases} \dfrac{\lambda - |d_p - \mu_0|}{\lambda^2} & \text{if } |d_p - \mu_0| < \lambda \\ 0 & \text{otherwise} \end{cases} \tag{95}$$

The analytical solution of Eq. (91) for the above-mentioned growth and attrition rates is obtained as a parameterized equation by using the Method of Characteristics (Ramkrishna, 2000):

$$n(t) = n_0(d_{p_0})e^{\frac{G_0'}{d_{p_{crit}}}t} \tag{96}$$

$$d_p(t) = d_{p_{crit}} + (d_{p_0} - d_{p_{crit}})e^{-\frac{G_0'}{d_{p_{crit}}}t} \tag{97}$$

Similarly to Case 2, since only growth or attrition occurs, N remains equal to its initial value N_0:

$$N\big|_{balance} = N_0 \tag{98}$$

The total particle volume V changes due to Q_{growth}. To be consistent with the mass balance, Q_{growth} must be given by:

$$Q_{growth} = \frac{\pi}{2}\int_0^\infty [G(d_p) - A(d_p)]n(d_p,t)d_p^2 dd_p \tag{99}$$

By replacing Eq. (92) in (99):

$$\begin{aligned} Q_{growth} &= \frac{\pi}{2}\int_0^\infty G_0'\left(1 - \frac{d_p}{d_{p_{crit}}}\right)n(d_p,t)d_p^2 dd_p \\ &= \frac{\pi}{2}G_0'\left(\mu_2 - \frac{\mu_3}{d_{p_{crit}}}\right) \end{aligned} \tag{100}$$

To analytically calculate the total particle volume, the three first moment equations must be solved. Then, from Eq. (5):

$$\frac{d\mu_1}{dt} = G_0'\left(\mu_0 - \frac{\mu_1}{d_{p_{crit}}}\right) \tag{101}$$

$$\frac{d\mu_2}{dt} = 2G_0'\left(\mu_1 - \frac{\mu_2}{d_{p_{crit}}}\right) \tag{102}$$

$$\frac{d\mu_3}{dt} = 3G_0'\left(\mu_2 - \frac{\mu_3}{d_{p_{crit}}}\right) \tag{103}$$

where the initial conditions (i.e., the population moments for $t = 0$) are computed by using Eqs. (4) and (95). After solving, the following analytical solution is obtained for μ_3.

$$\begin{aligned} \mu_3 = {} & d_{p_{crit}}^3 N_0 + 3d_{p_{crit}}^2(\mu_{10} - d_{p_{crit}}N_0)e^{-\frac{G_0't}{d_{p_{crit}}}} \\ & + 3d_{p_{crit}}(\mu_{20} - 2d_{p_{crit}}\mu_{10} + d_{p_{crit}}^2 N_0)e^{-\frac{2G_0't}{d_{p_{crit}}}} \\ & + (\mu_{30} - 3d_{p_{crit}}\mu_{20} + 3d_{p_{crit}}^2\mu_{10} - d_{p_{crit}}^3 N_0)e^{-\frac{3G_0't}{d_{p_{crit}}}} \end{aligned} \tag{104}$$

where $V\big|_{balance} = (\pi/6)\mu_3$.

Numerical simulations are performed for the discretization grids and parameter values shown in Table 1. Fig. 5 shows the analytical and numerical solutions obtained. The numerical method is able to predict the PSD with errors in the predictions of moments 0 and 3 lower than 0.001% and 0.2%, respectively; verifying the closure of the total number and volume balances. The numerical prediction of the PSD for $t = 300$ s, as shown in Fig. 5, is remarkable good considering that only four and six points have non-zero values for the arithmetic and geometric grids, respectively. Similarly to Case 2, when growth and attrition take place non-physical oscillations are not found.

5.4. Case 4

If only breakage in a steady-state continuous and perfectly mixed system takes place, Eq. (1) becomes:

$$\dot{n}_{in} - \dot{n}_{out} + h^{B+} - h^{B-} = 0 \tag{105}$$

where h^{B+} and h^{B-} are given by Eqs. (18) and (16). The breakage rate is assumed to be proportional to the particle size:

$$b = b_0 d_p \tag{106}$$

Besides, the following expression for the breakage probability function $P(d_p, x)$ is considered:

$$P(d_p, x) = \frac{1}{x} \tag{107}$$

Then, by using Eq. (19), the number of fragments given by the breakage of a particle of size x is:

$$\nu(x) = \frac{x^3}{\int_0^x P(d_p, x) d_p^3 dd_p} = 4 \tag{108}$$

In order to analytically solve Eq. (105), the number density function within the system is arbitrary proposed:

$$n = \frac{\dot{N}_{in}}{b_0 \bar{\mu}^2} e^{-\frac{d_p}{\bar{\mu}}} \tag{109}$$

where $\bar{\mu}$ is the arithmetic mean diameter of n. Assuming a mean residence time equal to $1/4b_0\bar{\mu}$, the density function of the solids outlet stream is given by:

$$\dot{n}_{out} = 4b_0 \bar{\mu} n \tag{110}$$

Using Eqs. (106)–(110) and the definitions h^{B+} and h^{B-}, the PSD for the inlet stream can be calculated by means of Eq. (105):

$$\dot{n}_{in} = \frac{\dot{N}_{in} d_p}{\bar{\mu}^2} e^{-\frac{d_p}{\bar{\mu}}} \tag{111}$$

The inlet volumetric flowrate is computed by multiplying Eq. (111) by $(\pi/6)d_p^3$ and integrating over the entire domain of sizes:

$$Q_{in} = 4\pi \quad \dot{N}_{in} \bar{\mu}^3 \tag{112}$$

The total particle number within the system is exactly calculated by integrating Eq. (109) over the entire size domain (moment 0):

$$N\big|_{balance} = \frac{\dot{N}_{in}}{b_0 \bar{\mu}} \tag{113}$$

The total particle volume remains constant; thus, at any time:

$$V\big|_{balance} = \frac{6\bar{\mu}^2 \dot{N}_{in}}{b_0} \tag{114}$$

In Fig. 6, the discrete number density values obtained by applying the proposed numerical method are compared with the analytical solution for the discretization grid and parameter values of Table 1. The results show that the numerical method is accurate. According to Table 1, moment 0 and 3 are satisfied, in fact numerical errors lower than 0.5 and 2×10^{-5}% are found, respectively.

5.5. Case 5

An analytical solution of the PBE for a perfectly mixed batch process with simultaneous growth and aggregation is available from Ramabhadran et al. (1976) and Qamar and Warnecke (2007). For this Case, Eq. (1) becomes:

$$\frac{\partial n}{\partial t} + G\frac{\partial n}{\partial d_p} = h^{A+} - h^{A-} \tag{115}$$

The mentioned authors proposed the following initial PSD:

$$n_0 = N_0 \frac{3d_p^2}{d_0^3} e^{-\left(\frac{d_p}{d_0}\right)^3} \tag{116}$$

N_0 is the initial total particle number and d_0 is the number–volume mean diameter of the initial PSD. Therefore, the initial total particle volume is:

$$V_0 = N_0 \frac{\pi}{6} d_0^3 \tag{117}$$

A constant value for the aggregation kernel is assumed. The rate of change of the particle volume is considered proportional to the particle volume (Ramabhadran et al., 1976; Qamar and Warnecke, 2007):

$$\frac{dV_p}{dt} = G_0'' V_p \tag{118}$$

Then, the growth rate is:

$$G = \frac{dd_p}{dt} = \frac{G_0''}{3} d_p \tag{119}$$

where G_0'' is a proportionality constant. To be consistent with the mass balance, the volumetric flowrate fed to the system that contributes to particle growth must satisfy Eq. (9). By replacing Eq. (119) in (9) and solving:

$$Q_{growth} = G_0'' V \tag{120}$$

Eq. (120) indicates that Q_{growth} must be proportional to the total particle volume within the system. The mass balance for this case becomes:

$$\frac{dV}{dt} = Q_{growth} = G_0'' V \tag{121}$$

By solving Eq. (121), the analytical solution for the total particle volume is obtained:

$$V\big|_{balance} = V_0 e^{G_0'' t} \tag{122}$$

The solution for the total particle number is given by Ramabhadran et al. (1976) and Qamar and Warnecke (2007):

$$N\big|_{balance} = \frac{2N_0}{2 + \beta N_0 t} \tag{123}$$

Besides, the analytical solution for n is:

$$n = 3\frac{N^2}{V} d_p^2 e^{-\frac{N}{V} d_p^3} \tag{124}$$

Fig. 7 shows the initial PSD and the numerical and analytical PSDs resulting from growth and aggregation for the discretization grids and parameter values of Table 1. The numerical solutions are in well agreement with the analytical ones and the errors in the predictions of moments 0 and 3 are lower than 0.1% and 1%, respectively. As observed for Case 1, the use of Eq. (68) to continuously update the representative diameter of each class successfully tracks the size of newborn particles by aggregation when growth also occurs. Therefore, the novel discretization strategy proposed for the growth/attrition terms and the moving pivot technique of Kumar and Ramkrishna (1996b), which have been developed separately, are consistently coupled here to give the whole numerical method is able to predict correctly the PSDs preserving the two desired population moments.

5.6. Case 6

An analytical solution for the PBE in a perfectly mixed batch process with simultaneous aggregation and breakage is available from Patil and Andrews (1998) and Lage (2002). For Case 6, the PBE becomes:

$$\frac{\partial n}{\partial t} = h^{B+} - h^{B-} + h^{A+} - h^{A-} \tag{125}$$

These authors proposed the following breakage probability function:

$$P(d_p, x) = \frac{3d_p^2}{x^3} \tag{126}$$

Therefore, the number of particles born by breakage is given by:

$$\nu(x) = \frac{x^3}{\int_0^x \frac{3d_p^2}{x^3} d_p^3 dd_p} = \frac{x^6}{3\int_0^x d_p^5 dd_p} = \frac{x^6}{3\frac{x^6}{6}} = 2 \tag{127}$$

Thus, it is assumed that each particle breaks into two fragments. As additional conditions, the breakage rate is considered proportional to the particle volume:

$$b = b_0' \frac{\pi}{6} d_p^3 \tag{128}$$

where b_0' is a constant. In addition, a constant value for the aggregation kernel is assumed.

For the available analytical solution, the selected initial PSD is:

$$n_0 = \frac{\pi}{2}\frac{N_0^2}{V_0} d_p^2 e^{-\frac{N_0}{V_0}\frac{\pi}{6}d_p^3} \tag{129}$$

For the conditions above detailed, the analytical solution is (Patil and Andrews, 1998; Lage, 2002):

$$n = \frac{\pi}{2}\frac{N^2}{V} d_p^2 e^{-\frac{N}{V}\frac{\pi}{6}d_p^3} \tag{130}$$

The total particle number is obtained by replacing Eq. (130) in (4) for $j=0$ and solving:

$$N\Big|_{balance} = \sqrt{\frac{2b_0'V}{\beta}}\left[\frac{1+\frac{1}{N_0}\sqrt{\frac{2b_0'V}{\beta}}\tan h\left(\sqrt{\frac{b_0'\beta V}{2}}t\right)}{\frac{1}{N_0}\sqrt{\frac{2b_0'V}{\beta}}+\tan h\left(\sqrt{\frac{b_0'\beta V}{2}}t\right)}\right] \tag{131}$$

The total particle volume remains equal to the initial one (only aggregation and breakage occur):

$$V\Big|_{balance} = V_0 \tag{132}$$

In Fig. 8, the calculated discrete values of number density function are compared with the analytical solution for the parameter values and discretization grids listed in Table 1. The numerical method is able to predict satisfactorily the PSDs satisfying the total number and volume balances (according to Table 1, the numerical errors for the predictions of moments 0 and 3 are lower than 0.26% and 0.003%, respectively). The updating strategy to calculate the representative diameters of each class (Eq. (68)) is also satisfactory when both agglomeration and breakage takes place.

5.7. Case 7

In this case, only attrition in a perfectly mixed steady-state continuous system is considered. Besides, a constant value for the attrition rate is assumed. Then Eq. (1) becomes:

$$-A\frac{dn}{dd_p} = \dot{n}_{in} - \dot{n}_{out} \tag{133}$$

$\dot{n}_{out}$ is computed by means of Eq. (74).

Eq. (133) is integrated to obtain:

$$n = \frac{e^{\frac{d_p}{A\tau}}}{A}\int_{d_p}^{\infty} \dot{n}_{in} e^{-\frac{d_p}{A\tau}} dd_p \tag{134}$$

For the inlet PSD, the following function is proposed:

$$\dot{n}_{in} = \dot{N}_{in}\frac{d_p}{d_{p0}^2} e^{-\frac{d_p}{d_{p0}}} \tag{135}$$

By replacing Eq. (135) in (134), the PBE solution is obtained:

$$n = \dot{N}_{in}\tau\frac{d_p d_{p0} + (d_p + d_{p0})A\tau}{d_{p0}(A\tau + d_{p0})^2} e^{-\frac{d_p}{d_{p0}}} \tag{136}$$

Applying the definition of population moment (Eq. (4)) to the analytical solution for $j=0$ and $j=3$, expressions for the total particle number and volume are respectively found:

$$N\Big|_{balance} = \frac{\dot{N}_{in}\tau d_{p0}(d_{p0}+2A\tau)}{(A\tau + d_{p0})^2} \tag{137}$$

$$V\Big|_{balance} = \frac{\pi\dot{N}_{in}\tau d_{p0}^4(24d_{p0}+30A\tau)}{6(A\tau + d_{p0})^2} \tag{138}$$

Although the only size change mechanism is attrition, the equation predicts a decrease in the total particle number. This is because the particles that shrink until $d_p = 0$ disappear. Then, this case combines particle size reduction with disappearance.

For the discretization grid and parameter values of Table 1, Fig. 9 shows the analytical and numerical solutions three simulation tests. The numerical solutions are in good agreement with the analytical ones, being the errors in the predictions of moments 0 and 3 lower than 0.5% and 1%, respectively.

5.8. Case 8

In this Case, the PBE for a process with simultaneous growth and nucleation in a batch perfectly mixed system is solved. Constant values for the growth and nucleation rates are assumed. Then, Eq. (1) becomes:

$$\frac{\partial n(d_p,t)}{\partial t} + G\frac{\partial n(d_p,t)}{\partial d_p} = B_{nuc}\delta(d_p - d_{nuc}) \tag{139}$$

The analytical solution of Eq. (139) is obtained by using the Method of Characteristics:

$$n = n_0(d_p - Gt) + \frac{B_{nuc}}{G} Heaviside\left(t - \frac{d_p - d_{nuc}}{G}\right) \tag{140}$$

The selected initial PSD is:

$$n_0 = N_o\frac{3d_p^2}{d_0^3} e^{-\left(\frac{d_p}{d_{nv}}\right)^3} \tag{141}$$

where d_{nv} is the number–volume mean diameter of the initial PSD. By replacing Eq. (141) in (140), the analytical solution becomes:

$$n = N_o\frac{3(d_p - Gt)^2}{d_0^3} e^{-\left(\frac{d_p - Gt}{d_0}\right)^3} + \frac{B_{nuc}}{G} Heaviside\left(t - \frac{d_p - d_{nuc}}{G}\right) \tag{142}$$

The total particle number and volume are respectively:

$$N\Big|_{balance} = N_o + B_{nuc}t \tag{143}$$

$$V\Big|_{balance} = V_o + \int_0^t Q_{growth}dt + \frac{B_{nuc}G^3t^4}{4} \tag{144}$$

Q_{growth} is obtained from Eq. (9):

$$G = \frac{2Q_{growth}}{\pi\ \mu_2} \tag{145}$$

Eq. (145) indicates that Q_{growth} must change with time proportionally to μ_2. By replacing Eq. (145) in (144):

$$V\Big|_{balance} = V_o + \frac{\pi}{2}G\int_0^t \mu_2 dt + \frac{B_{nuc}G^3t^4}{4} \tag{146}$$

Simulations are performed using the discretization grid and parameter values listed in Table 1. In Fig. 10, the predicted values by using the proposed numerical method are compared to the analytical solution. The results show that the proposed method works properly to predict the distributions despite the sharp fronts exhibited by the PSDs. Nonetheless, it is worth to mention that there is an overestimation of the density function in the edge of the growing front of nucleated particles. This numerical deviation is visible because the analytical solution for nucleation is a horizontal straight line. However, this deviation is only 2% from the analytical value.

Table 1 indicates that the population moments 0 and 3 are well predicted with errors lower than 0.01% and 0.7%, respectively. This result reinforces the advantage of the proposed method to handle any kind of size change mechanism and PSDs shape. The good

predictions are attributed to two main characteristics of the numerical technique: (a) the ability to satisfy moments 0 and q for each class and consequently for the entire population and (b) the representative class size updating strategy to numerically capture the newborn particles by nucleation.

6. Conclusions

The relatively simple proposed numerical technique is able to solve PBEs using any type of discretization grid (e.g., geometrical, arithmetical) with different coarseness and number of classes. The original contributions of this work are:

- The discretization performed for the growth and attrition terms, in which a linear approximation for the density function within each class is considered to estimate the convective fluxes at the cell boundaries. On the other hand, the fluxes are split in positive and negative contributions (i.e., growth or attrition); the flux at each class boundary is calculated once the upwind direction is available. For PBEs including growth and/or attrition terms, the discretization technique is able to overcome the commonly found numerical difficulties. The novel approach to represent the density number function within each size class allows describing the particle number flux between nodes properly. Thus, the numerical diffusion is significantly minimized. Moreover, the method is efficient in predicting steep moving fronts that might appear in PSDs. The performed simulations and the comparison with analytical solutions indicate that the numerical technique is capable to solve the PBE despite its hyperbolic nature, minimizing the broadening tendency of sharp discontinuities. Furthermore, for growth processes, the numerical solutions do not show non-physical oscillations, demonstrating that numerical dispersion is also minimized. The updating strategy proposed to calculate the representative size classes also allows achieving good closure of the population moments even for complex size change kinetic laws.
- The coupling between the moving pivot technique of Kumar and Ramkrishna (1996b) and the discretization proposed for the growth and attrition terms. The usage of a linear density function, which is consistent with the same two population moments conserved by the pivot moving discretization, allows preserving the sectional and global population moments even when all the size change mechanisms occur simultaneously.
- The combination between the moving pivot technique (Kumar and Ramkrishna, 1996b) and the cell-average technique (Kumar et al., 2006) introduced to conserve the desired sectional population moments without redistribution of newly born particles.

The testing results indicate that the proposed method was capable to properly handle any kind of size change mechanism, either alone or in combination, and different initial or inlet PSD shapes, even those having steep fronts and/or sharp discontinuities. The good predictions are attributed to two main characteristics of the numerical technique: (a) the ability to satisfy moments 0 and q (arbitrarily selected) for each class (sectional moments) and consequently for the entire population and (b) the representative class-size updating strategy to numerically capture newborn particles. This approach avoids the reassignment of newborn particles to existing predefined sizes and the need of adding or subtracting classes to keep constant the grid density.

Since the numerical method solves two differential equations per class, it is expected that the method is less computationally efficient than those methods that use only one equation per class (e.g., the Fixed Pivot technique of Kumar and Ramkrishna (1996a) and the Cell Average method of Kumar et al. (2006)). For pure aggregation and/or brakeage processes, since the proposed method matches the Moving Pivot technique of Kumar and Ramkrishna (1996b), simulations are carried out with the same computational demands that the Moving Pivot method. Moreover, since the moving pivot discretization results in a stiff differential equations system, the set of ordinary differential equations (ODEs) requires a stiff solver. In this work, the model code is implemented in FORTRAN programming language by means of a Gear subroutine, and no robustness problems are found to solve the ODEs.

When only growth and/or attrition mechanisms occur, the PBE is solved much faster than for pure aggregation problems because there is no need to evaluate double summations. On the other hand, the proposed method is more robust than other techniques that show oscillations and give incorrect predictions of the PSDs (e.g., the Hounslow discretization, 1988).

Expanding the proposed numerical technique to solve multivariate PBEs is the subject for future work.

References

Abberger T. The effect of powder type, free moisture and deformation behaviour of granules on the kinetics of fluid-bed granulation. Eur J Pharm Biopharm 2001;52:327–36.

Alexopolous AH, Roussos AI, Kiparissides C. Part II: Dynamic evolution of the particle size distribution in particulate processes undergoing simultaneous particle nucleation, growth and aggregation. Chem Eng Sci 2005;59:5751–69.

Allen T. Powder sampling and particle size determination. Amsterdam, The Netherlands: Elsevier; 2003.

Bajcinca N, Hofmann S, Sundmacher K. Method of moments over orthogonal polynomial bases. Chem Eng Sci 2014;119:295–309.

Bucalá V, Piña J. Teaching population balances for chemical engineering students, application to granulation processes. Chem Eng Educ 2007;41(3):209–17.

Cameron IT, Wang FY, Immanuel CD, Stepanek F. Process systems modelling and applications in granulation: a review. Chem Eng Sci 2005;60(14):3723–50.

Durran DR. Numerical methods for fluid dynamics. New York: Springer; 2010.

Gerstlauer A, Gahn C, Zhou H, Rauls M, Schreiber M. Application of population balances in the chemical industry – current status and future needs. Chem Eng Sci 2006;61:205–17.

Gunawan R, Fusman I, Braatz D. High resolution algorithms for multidimensional population balance equations. AIChE J 2004;50(11):2738–49.

Holdich RG. Fundamentals of particles technology. England: Midland Information Technology & Publishing; 2002.

Hounslow MJ. Discretized population balance for continuous systems at steady state. AIChE J 1990;36(1):106–16.

Hounslow MJ, Ryall RL, Marshall VR. Discretized population balance for nucleation, growth and aggregation. AIChE J 1988;34(11):1821–32.

Hulburtz HM, Katz SL. Some problems in particle technology: a statistical mechanical formulation. Chem Eng Sci 1964;19:555–74.

Kayaert AF, Antonus, RAC. Process for the production of urea granules. US Patent 5653781; 1997.

Kiparissides C. Challenges in particulate polymerization reactor modeling and optimization: a population balance perspective. J Process Control 2006;16:205–24.

Kruis FE, Maisels A, Fissan H. Direct simulation Monte Carlo method for particle coagulation and aggregation. AIChE J 2000;46(9):1735–42.

Kumar S, Ramkrishna D. On the solution of population balance equations by discretization: I. A fixed pivot technique. Chem Eng Sci 1996a;51(8):1311–32.

Kumar S, Ramkrishna D. On the solution of population balance equations by discretization: II. A moving pivot technique. Chem Eng Sci 1996b;51(8):1333–42.

Kumar S, Ramkrishna D. On the solution of population balance equations by discretization: III. Nucleation, growth and aggregation of particles. Chem Eng Sci 1997;52(24):4659–79.

Kumar J. [PhD thesis] Numerical approximations of population balance equations in particulate systems [PhD thesis]. Magdeburg: Faculty of Mathematics, Otto-von-Guericke University; 2006.

Kumar J, Peglow M, Warnecke G, Heinrich S, Mörl L. Improved accuracy and convergence of discretized population balance for aggregation: the cell average technique. Chem Eng Sci 2006;61:3327–42.

Lage PLC. Comments on the analytical solution to continuous population balance equation with coalescence and breakage – the special case with constant number of particles. Chem Eng Sci 2002;57:4253–4.

Lee K, Matsoukas T. Simultaneous coagulation and break-up using constant-*N* Monte Carlo. Powder Technol 2000;110:82–9.

Leturia M. [PhD thesis] Étudehydrodynamique et Modélisation des Réacteurs de Carbochloration [PhD thesis]. Université de Compiegne; 2013.

LeVeque RJ. Finite volume methods for hyperbolic problems. UK: Cambridge University Press; 2002.

Lin Y, Lee K, Matsoukas T. Solution of the population balance equation using constant-*N* Monte Carlo. Chem Eng Sci 2002;57:2241–52.

Ma DL, Tafti DK, Braatz RD. High resolution simulation of multidimensional crystal growth. Ind Eng Chem Res 2002;41:6217–23.

Madras G, McCoy BJ. Dynamics of crystal size distributions with size-dependent rates. J Cryst Growth 2004;243:204–13.
Majumder A, Kariwala V, Ansumali S, Rajendran A. Fast high-resolution method for solving multidimensional population balances in crystallization. Ind Eng Chem Res 2010;49:3862–72.
Marchal P, David R, Klein JP, Villermaux J. Cristallization and precipitation engineering: I. An efficient method for solving population balance in crystallization with aggregation. Chem Eng Sci 1988;43(1):59.
Marchisio DL, Fox RO. Solution of population balance equations using the direct quadrature method of moments. J Aerosol Sci 2005;36:43–73.
Maurstad O. [PhD thesis] Population balance modeling of aggregation in granulation processes [PhD thesis]. Norwegian: University of Science and Technology; 2002.
Mesbah A, Kramer HJM, Huesman AEM, Van den Hof PMJ. A control oriented study on the numerical solution of the population balance equation for crystallization processes. Chem Eng Sci 2009;64:4262–77.
Motz S, Mitrovic A, Gilles E-D. Comparison of numerical methods for the simulation of dispersed phase systems. Chem Eng Sci 2002;57:4329–44.
Mörl L, Heinrich S, Peglow M. Fluidized bed spray granulation. In: Salman AD, Hounslow MJ, Seville JPK, editors. Handbook of powder technology. Amsterdam, The Netherlands: Elsevier; 2007.
Nopens I, Beheydt D, Vanrolleghem PA. Comparison and pitfalls of different discretised solution methods for population balance models: a simulation study. Comput Chem Eng 2005;29(2):367–77.
Nopens I, Vanrolleghem PA. Comparison of discretization methods to solve a population balance model of activated sludge flocculation including aggregation and breakage. Math Comput Model Dyn Syst 2006;12(5):441–54.
Patil DP, Andrews JRG. An analytical solution to continuous population balance model describing floc coalescence and breakage – a special case. Chem Eng Sci 1998;53(3):599–601.
Pilon L, Viskanta R. Modified method of characteristics for solving population balance equations. Int J Numer Methods Fluids 2003;42:1211–36.
Pinto MA, Immanuel CD, Doyle FJ III. A two-level discretisation algorithm for the efficient solution of higher-dimensional population balance models. Chem Eng Sci 2008;63:1304–14.
Pulliam TH, Zingg DW. Fundamental algorithms in computational fluid dynamics. Springer; 2014.
Qamar S. [PhD thesis] Model and simulation of population balances for particulate processes [PhD thesis]. Magdeburg: Faculty of Mathematics, Otto-von-Guericke University; 2008.
Qamar S, Warnecke G. Numerical solution of population balance equations for nucleation, growth and aggregation processes. Comput Chem Eng 2007;31:1576–89.
Qamar S, Ashfaq A, Warnecke G, Angelov I, Elsner MP, Seidel-Morgenstern A. Adaptive high-resolution schemes for multidimensional population balances in crystallization processes. Comput Chem Eng 2007;31(10):1296–311.
Ramabhadran TE, Peterson TW, Seinfeld JH. Dynamics of aerosol coagulation and condensation. AIChE J 1976;22(5):840–51.
Ramachandran R, Barton PI. Effective parameter estimation within a multidimensional population balance model framework. Chem Eng Sci 2010;65:4884–93.
Ramkrishna D. Population balances. London, England: Academic Press; 2000.
Randolph AD, Larson MA. Theory of particulate processes. New York, USA: Academic Press; 1971.
Rigopoulos S, Jones AG. Finite-element scheme for solution of the dynamic population balance equation. AIChE J 2003;49(5):1127–39.
Rhodes M. Introduction to particle technology. West Sussex, England: Wiley; 2008.
Smith M, Matsoukas T. Constant-number Monte Carlo simulation of population balances. Chem Eng Sci 1998;53:1777–86.
Smith PG, Nienow AW. Particle growth mechanisms in fluidised bed granulation: I. The effect of process variables. Chem Eng Sci 1983;38(8):1223–31.
Strikwerda JC. Finite difference schemes and partial differential equations. 2nd ed. Philadelphia: Society for Industrial and Applied Mathematics (SIAM); 2004.
Sweby PK. High resolution schemes using flux limiters for hyperbolic conservation laws. SIAM J Numer Anal 1984;21(5):995–1011.
Utomo J, Zhang T, Balliu N, Tadé MO. Numerical studies of wavelet-based method as an alternative solution for population balance problems in a batch crystalliser. In: ADCHEM 2009, Koc University, Elsevier Ltd.; 2009.
Vanni M. Approximate population balance equations for aggregation–breakage processes. J Colloid Interface Sci 2000;221:143–60.
Wang Q, Luo Z, Ni M, Cen K. Particle population balance model for a circulating fluidized bed boiler. Chem Eng J 2003;93:121–33.